Synaptic Energy Use and Supply

Julia J. Harris,[1,2] Renaud Jolivet,[1,2] and David Attwell[1,*]
[1]Department of Neuroscience, Physiology & Pharmacology, University College London, Gower Street, London WC1E 6BT, UK
[2]These authors contributed equally to this work
*Correspondence: d.attwell@ucl.ac.uk
http://dx.doi.org/10.1016/j.neuron.2012.08.019

Neuronal computation is energetically expensive. Consequently, the brain's limited energy supply imposes constraints on its information processing capability. Most brain energy is used on synaptic transmission, making it important to understand how energy is provided to and used by synapses. We describe how information transmission through presynaptic terminals and postsynaptic spines is related to their energy consumption, assess which mechanisms normally ensure an adequate supply of ATP to these structures, consider the influence of synaptic plasticity and changing brain state on synaptic energy use, and explain how disruption of the energy supply to synapses leads to neuropathology.

The nervous system consumes a disproportionate fraction of the resting body's energy production: in humans the brain is only 2% of the body's mass, yet it uses ~20% of the O_2 consumed by the resting body (Mink et al., 1981), while the retina alone uses 10% of the fly's resting ATP consumption (Laughlin et al., 1998). The relative energy consumption of the brain has increased particularly during the evolution of humans from lower primates (Mink et al., 1981; Aiello and Wheeler, 1995), reflecting a 3-fold expansion in the size of the brain relative to the body and an increase in the number of synapses per cortical neuron (Abeles, 1991). This greater energy allocation to CNS tissue over millions of years underpins our brains' greater cognitive powers, and was made possible by an increased and higher-quality food intake, along with less energy expenditure on the gut and locomotion (Aiello and Wheeler, 1995; Navarrete et al., 2011). What is all this energy used for in the brain, how does it determine the brain's information processing power, and how does the brain's high energy use predispose it to problems when energy is not supplied at the necessary rate?

We will review how most brain energy is used on synapses, investigate how pre- and postsynaptic terminals are optimized to maximize information transmission at minimum energy cost, and assess how ATP provision to synapses is regulated to satisfy their energetic needs. We then consider how synapse energy use changes with development and synaptic plasticity, and between wake and sleep states, before relating how defects in synaptic energy supply can lead to disease.

Most Brain Energy Is Used on Synapses

The ATP consumption by the major subcellular processes underlying signaling in the brain (Figure 1) has been estimated for rat cerebral cortex (Attwell and Laughlin, 2001) and for human cortex (Lennie, 2003). Anatomical data on mean cell size, and the capacitance per area of membrane, were used to estimate the Na^+ that enters to produce action potentials and thus needs to be pumped out again by the Na^+/K^+-ATPase, consuming ATP. Similarly, patch-clamp data provided quantification of the ions entering to generate typical synaptic currents, which also need to be pumped out (for simplicity all neurons, rather than ~85% [Abeles, 1991], were assumed to be excitatory).

The ATP used on ion pumping maintaining the resting potential, and on biochemical pathways underlying synaptic transmitter and vesicle recycling, were also calculated. This analysis of where ATP is used suggested that electrical signaling processes are the major consumer of energy in the brain. Furthermore, the largest component of the signaling energy use is on synaptic transmission.

Figure 2A shows the predicted distribution of ATP use across the different signaling mechanisms in rat neocortex, updated from the earlier Attwell and Laughlin (2001) calculations by taking into account the fact that action potentials in mammalian neurons use less energy than Attwell and Laughlin (2001) assumed based on squid axon data (Alle et al., 2009; Carter and Bean, 2009; Sengupta et al., 2010; Harris and Attwell, 2012). These calculations predict that the pre- and postsynaptic mechanisms mediating synaptic transmission (including glutamate accumulation in vesicles) consume 55% of the total ATP used on action potentials, synaptic transmission, and the resting potentials of neurons and glia. This is equivalent to 41% of the total ATP used in the cortex if housekeeping energy use, on tasks like synthesis of molecules and organelle trafficking, uses 25% of the total energy (Attwell and Laughlin, 2001). The percentage of energy used on synapses may be even larger in the primate cortex, where the number of synapses per neuron is larger (Abeles, 1991). In contrast, the energy use of the white matter is 3-fold lower than the gray matter, mainly because it has an 80-fold lower density of synapses (Harris and Attwell, 2012). The distribution of ATP consumption across the various mechanisms contributing to synaptic transmission (Figure 2B) shows that reversing the ion movements generating postsynaptic responses consumes the great majority of the energy used (at excitatory synapses: inhibitory synapses are predicted to use much less energy to reverse postsynaptic Cl^- fluxes because the chloride reversal potential is close to the resting potential [Howarth et al., 2010]).

Figure 2C compares the predicted energy expenditure in the dendrites and soma, axons, and glia with the fraction of mitochondria observed in these locations by Wong-Riley (1989). The subcellular location of mitochondria reflects well the high predicted energy consumption of postsynaptic currents
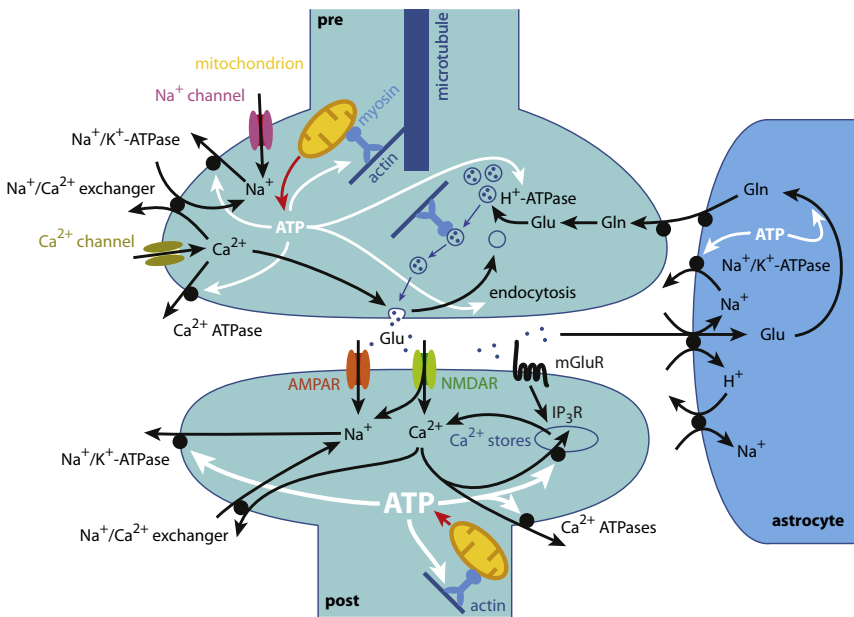
Figure 1. Mechanisms that Consume Energy at Synapses

ATP consumption by signaling mechanisms (Attwell and Laughlin, 2001). Presynaptically, ATP is used on four types of ATPase: the sodium pump, which extrudes Na^+ ions generating the action potential and powers Ca^{2+} removal by Na^+/Ca^{2+} exchange; calcium-ATPase in the plasma membrane (and endoplasmic reticulum, not shown), which lowers $[Ca^{2+}]_i$; vacuolar H^+-ATPase, which energizes vesicle transmitter uptake; and motor proteins (kinesin, dynein, myosin) that move mitochondria and vesicles around the cell. In addition, vesicle retrieval by dynamin consumes GTP. Postsynaptically, ATP use is larger (shown by thicker arrows) and is mainly on the pumping out of ions mediating synaptic currents, with a smaller usage on returning Ca^{2+} to intracellular stores and on mitochondrial trafficking. In astrocytes ATP is used largely on extruding Na^+, to maintain the resting potential and to remove the ions driving glutamate uptake, and on conversion of glutamate into glutamine. A small amount of energy (not included here) may also be consumed by signaling mediated by ATP.

(Figure 2A). The fraction of energy expenditure predicted for axons and synaptic terminals is lower than the fraction of mitochondria observed in those areas, perhaps implying that there is some energy consuming presynaptic process that is unaccounted for (possibly vesicle trafficking: Verstreken et al., 2005), while the predicted astrocyte energy use is substantially larger than the fraction of mitochondria observed in astrocytes, possibly because astrocytes are more glycolytic than neurons.

Since synapses use such a large fraction of the brain's energy, we might expect evolution to have optimized their function to maximize the information they transmit while minimizing their energy use, in order to reduce the ATP consumption of neural circuits. Based on this idea, in the following sections we present some "energetic design principles" for presynaptic terminals and postsynaptic spines.

The Energy Cost of Synaptically Transmitting One Bit of Information

First, we estimate how much ATP is needed to transmit information across a single synapse, as a prelude to explaining how the information transmitted can be maximized at minimum energy cost. The input to a synapse can be considered over a sequence of time intervals, Δt, in which an action potential either does or does not arrive along the axon, e.g., signifying the presence or absence of some stimulus (Figure 3A, Δt is the smallest interval over which the neuron can represent information, set by the refractory period of the action potential). If the mean spike firing rate is S, the probability of an action potential arriving in any given interval is $s = S\Delta t$ (with $0 < s < 1$), and we assume no correlation between the occurrence of different action potentials, the rate at which information arrives in the input train is (Shannon, 1948; Dayan and Abbott, 2001, Equation 4.4; Levy and Baxter, 1996, Equation 2.1)

$$I_{input}(s) = -s \cdot \log_2(s) - (1-s) \cdot \log_2(1-s) \qquad (1)$$

bits per Δt (Figure 3A). This is maximized with $s = 0.5$, or $S = 1/(2\Delta t)$, i.e., with the neuron firing at half its maximum rate. This is ~ 200 Hz for a refractory period of $\Delta t = 2.5$ ms, yet in practice the mean firing rate of neurons in vivo is much lower than this, around 4 Hz (Attwell and Laughlin, 2001; Perge et al., 2009). To explain this difference, Levy and Baxter (1996) suggested that, in fact, the nervous system maximizes the ratio of information transmitted to energy consumed (rather than maximizing coding capacity). They showed that, if the energy use of a neuron (and associated glia) is r-fold higher when producing a spike than when inactive, then the spike probability (s^*) that maximizes the information transmitted per energy consumed is much lower than that which would maximize information coding capacity. Their analysis implies that the factor, r, by which spiking increases energy use is related to s^* via the equation

$$r = \frac{\log_2(s^*)}{\log_2(1-s^*)}, \qquad (2)$$

which we use below. Applying similar principles to the transmission of information through a synapse leads to the surprising conclusion that the energetic design of synapses is optimized if presynaptic release of transmitter fails often—just as is seen in most synapses. To understand this we need to consider information flow through synapses and the energy it consumes.

For a synapse with a single release site (e.g., to the orange cell in Figure 3), if each time a presynaptic action potential arrives a vesicle is released with probability p, then for $p < 1$ information is lost during synaptic transmission. This is because, while the occurrence of a postsynaptic current tells the postsynaptic cell that there definitely was a presynaptic action potential (ignoring spontaneous vesicle release which will be considered below), if no current occurs that may be due either to no presynaptic action potential occurring or alternatively due to an action potential failing to evoke transmitter release. The amount of information passing through the synapse can be measured as
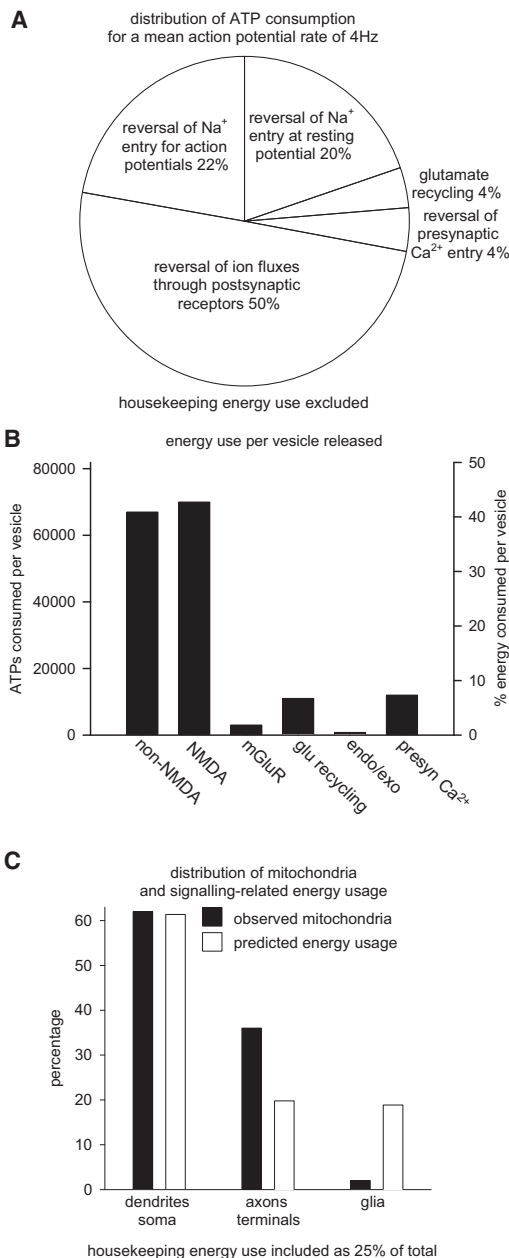
A

distribution of ATP consumption
for a mean action potential rate of 4Hz

housekeeping energy use excluded

B

C

housekeeping energy use included as 25% of total

Figure 2. Energy Consumption of Different Signaling Mechanisms
(A) Percentage of ATP predicted to be used on the subcellular mechanisms of Figure 1, from the analysis of Attwell and Laughlin (2001), updated to account for mammalian action potentials using less energy than those in squid giant axon.
(B) The energy per vesicle released expended on different aspects of excitatory synaptic transmission (postsynaptic non-NMDA, NMDA, and metabotropic glutamate receptors; recycling of glutamate [glu], endo- and exocytosis of vesicles [endo/exo], and presynaptic Ca^{2+} entry) expressed as ATP molecules (left ordinate) or percentage (right ordinate). See Attwell and Laughlin (2001) for the derivation of these numbers.
(C) Distribution of mitochondria in different subcellular compartments observed by Wong-Riley (1989) in primate visual cortex, compared with the predicted distribution of energy expenditure from (A) with housekeeping energy added as 25% of the total (allocated in proportion to the volume of the different compartments, using neuronal dimensions from Attwell and Laughlin (2001) and an astrocyte volume of 1.49×10^{-14} m³ (Chvátal et al., 2007).

the so-called mutual information, i.e., how much the sequence of postsynaptic currents (EPSCs) tells us about the input train of action potentials (APs), which is calculated (see Figure 3B legend) in bits per Δt as

$$I_m(\text{EPSCs; APs}) = I_{input}(s) + (1 - s) \cdot \log_2\left(\frac{(1 - s)}{(1 - p \cdot s)}\right)$$
$$+ s \cdot (1 - p) \cdot \log_2\left(\frac{s \cdot (1 - p)}{(1 - p \cdot s)}\right) \quad (3)$$
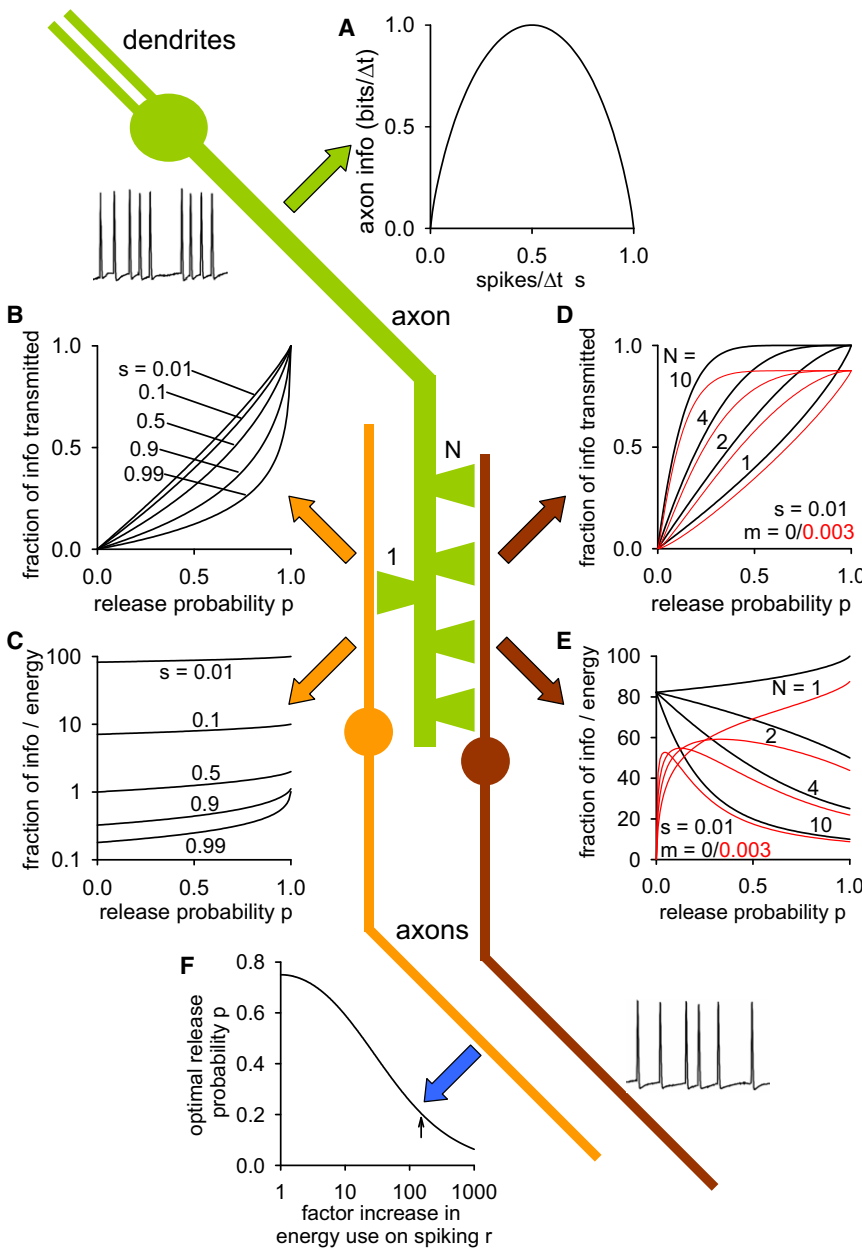
where s is again the probability of a spike arriving within Δt. The sum of the last two terms is negative and decreases the transmitted information below the input information defined in Equation 1. Equation 3 is plotted in Figure 3B for various values of s, normalized to the information in the incoming action potential stream in Equation 1 above, to show the fraction of incident information that is transmitted to the postsynaptic cell by the synapse. To assess the energetic efficiency of this information transfer (Laughlin et al., 1998; Balasubramanian et al., 2001), Figure 3C shows the ratio of the fraction of information emerging from the synapse to the energy consumed, which we take as being proportional to the rate of vesicle release, $s \cdot p$ (see figure legend).

As an example of the energetic cost of information transmission through synapses, if we set typical physiological values of $s = 0.01$ (implying a firing rate of $S = 4$ Hz) and $p = 0.25$, Equation 3 states that, out of the 32 bits/s arriving at the synapse, 6.8 bits/s are transmitted, and from the estimate by Attwell and Laughlin (2001) of the underlying synaptic energy cost ($E_{vesicle} = 1.64 \times 10^5$ ATP molecules per vesicle released), this is achieved at a cost of $S \cdot p \cdot E_{vesicle} = 1.64 \times 10^5$ ATP/s. Thus, information transmission typically costs ~24,000 ATP per bit, similar to the estimate of Laughlin et al. (1998). Increasing the release probability to 1 leads to an information transmission rate of 32 bits/s, at a cost of 20,500 ATP/bit.

Optimal Energetic Design of CNS Synapses Requires Failures of Presysynaptic Release
Both the fraction of information transmitted and the information transmitted per energy used are maximized when the release probability is 1 (Figures 3B and 3C). Why then do CNS synapses typically have a release probability of 0.25–0.5 (Attwell and Laughlin, 2001)? In this section we show that a low release probability can maximize the ratio of information transmitted to ATP used.

It has been suggested that a low release probability allows synapses to have a wide dynamic range, increases information transmission from correlated inputs, or maximizes information storage (Zador, 1998; Goldman, 2004; Varshney et al., 2006). However, two energetic aspects of synaptic function also benefit from a low release probability. First, considering the influence of a single axon on a postsynaptic neuron, the existence of multiple synaptic release sites (usually onto different spines), at each of which a vesicle is released with probability p onto the postsynaptic cell (as for the brown cell in Figure 3), results in the ratio of information transmitted to energy used being larger if the release probability is low (see below). Second, if the rate at which information arrives in all the synapses impinging on the dendritic tree is matched to the rate at which the output axon of the cell can convey information, this also implies that synaptic failures should occur (Levy and Baxter, 2002).

Figure 3. Energy Limitations Imply that Synaptic Failures Are Desirable

Information flow from an input neuron (green) through a single synapse (to the orange neuron) or multiple synapses (to the brown neuron).

(A) Information transmitted along the input axon per time Δt (from Equation 1) is maximized at 1 bit/Δt when s, the probability of an action potential/Δt, is 0.5.

(B) Fraction of information arriving on the axon that is transmitted across a synapse releasing one vesicle with probability p, calculated as the mutual information

$$I_m = I_{input}(s) + \sum_y P[y] \cdot \sum_x P[x|y] \cdot \log_2(P[x|y])$$

(where the input x is 1 when there is a spike and 0 otherwise, the output y is 1 when there is an EPSC and 0 otherwise, and the sum is over all x and y [Dayan and Abbott, 2001, Equation 4.12], which gives Equation 3), divided by the input information $I_{input}(s)$ in Equation 1.

(C) Ratio of information fraction transmitted (from B) to energy used on synaptic transmission, taken as $s \cdot p$, the number of vesicles released per Δt, assuming that energy use is proportional to the number of vesicles released, with release of one vesicle consuming one unit of energy (if the small percentage (~7%, Figure 2B) of ATP used on presynaptic Ca^{2+} pumping varies more weakly than p, the curves will decrease more as p approaches zero).

(D) Fraction of information arriving on an axon that is transmitted across N synapses each releasing one vesicle with probability p, in the absence of spontaneous release (Equation 4, black lines), and in the presence of mEPSCs occurring in the whole cell with a probability $m = 0.003$ per Δt (Equation 5, red).

(E) Ratio of information fraction transmitted (from D) to postsynaptic energy used, taken as $N \cdot s \cdot p$ (the number of vesicles released by action potentials per Δt), in the absence (black) and presence (red) of spontaneous release.

(F) Dependence on the factor r, by which spiking increases energy use, of the release probability that matches output information rate to the information arriving on a large number of independent input synapses (from Levy and Baxter, 2002). From Figure 2, per $\Delta t = 2.5$ ms, resting potentials and housekeeping use 3×10^6 ATP, while an

action potential (and downstream synaptic events) uses 4.5×10^8 ATP and increases energy use $r = 150$-fold (arrow). For $r = 150$, Equation 2 predicts an optimal spike probability, to maximize axonal information transmission/energy used, of $s^* = 0.024$ (a firing rate of 9.7 Hz) and the graph predicts $p \sim 0.2$.

Taking first the issue of several (N) synaptic release sites from one axon onto a postsynaptic cell, we define a response in the postsynaptic cell as occurring whenever it receives at least one synaptic current. (Because we are only considering information transfer across the synapse, i.e., determining how much the arrival of EPSCs in the postsynaptic cell tells that cell about the presynaptic input spike train, the amplitude of the EPSC in the postsynaptic cell is immaterial [although its size may determine how it affects the firing of the postsynaptic cell].) If we ignore postsynaptic noise and variability in the currents evoked by different vesicles, then the information received by the postsynaptic cell (i.e., the mutual information between the occurrence of responses in the postsynaptic cell and the action potentials arriving with probability s in each interval Δt, see Figure 3B legend) is given by

$$I_m = I_{input}(s) + (1-s) \cdot \log_2\left(\frac{(1-s)}{\left[1-s+s\cdot(1-p)^N\right]}\right)$$

$$+ s\cdot(1-p)^N \cdot \log_2\left(\frac{s\cdot(1-p)^N}{\left[1-s+s\cdot(1-p)^N\right]}\right)$$

(4)

bits per Δt. The number of release sites, N, varies (Zador, 2001), but is often greater than 1, e.g., more than 6 for cortical pyramidal to interneuron synapses (Deuchars and Thomson, 1995), 4–6 for spiny stellate and pyramidal cell to pyramidal cell synapses in cortex (Markram et al., 1997; Silver et al., 2003), and ~6 for excitatory synapses onto pyramidal cells in hippocampal area CA1 (Larkman et al., 1997). This multiplicity of synaptic release sites in parallel, usually onto different spines, may exist to ensure stable information processing in the face of spine turnover (Xu et al., 2007). Figure 3D (black lines) shows the fraction of the axonal input information that is transmitted to the postsynaptic cell, for various numbers of release sites (with the same release probability p), and for s set to 0.01 implying a firing rate of ~4 Hz for Δt = 2.5 ms (higher values of firing rate give curves that are similar in shape). Having several synaptic release sites ($N > 1$) from the axon to the receiving neuron increases the reliability of transmission, so that a larger fraction of the input information is received postsynaptically (de Ruyter van Steveninck and Laughlin, 1996; Manwani and Koch, 2001; Zador, 2001). However, as shown from the black lines in Figure 3E, for $N > 1$ it is no longer the case that the information transmitted per energy used is maximal with a release probability of 1; indeed, the highest ratio of information transmission to energy used is with p very low. For example, Figure 3D shows that for $N = 4$ synaptic release sites from each axon onto the postsynaptic cell, a release probability of $p = 0.25$ transmits over 60% of the information that would occur with $p = 1$, yet it uses only 25% of the energy to do so (since only 1/4 the number of vesicles are released).

Surprisingly, the preceding analysis predicts the greatest energy efficiency (information transmitted/energy used) for convergent synapses if they have zero release probability (Figure 3E). A more realistic result is obtained if it is recognized that the postsynaptic neuron will also experience a low rate of spontaneous vesicle release from all its input synapses (i.e., miniature synaptic currents at a total rate of m per Δt), each of which produces a postsynaptic effect indistinguishable from the action potential evoked release of one vesicle. In this case Equation 4 becomes

$$
\begin{aligned}
I_m = I_{input}(s) + (1-m) \cdot \Bigg\{ & (1-s) \cdot \log_2\left(\frac{(1-s)}{\left[1-s+s\cdot(1-p)^N\right]}\right) \\
& + s\cdot(1-p)^N \cdot \log_2\left(\frac{s\cdot(1-p)^N}{\left[1-s+s\cdot(1-p)^N\right]}\right) \Bigg\} \\
& + (1-s)\cdot m \cdot \log_2\left\{\frac{(1-s)\cdot m}{\left[m+s\cdot(1-m)\cdot\left(1-(1-p)^N\right)\right]}\right\} \\
& + s\cdot\left[1-(1-p)^N\cdot(1-m)\right]\cdot \\
& \quad \log_2\left\{\frac{s\cdot\left[1-(1-p)^N\cdot(1-m)\right]}{\left[m+s\cdot(1-m)\cdot\left(1-(1-p)^N\right)\right]}\right\}
\end{aligned}
\tag{5}
$$

The presence of spontaneous release decreases the maximum information transmittable (red curves in Figure 3D) because some postsynaptic currents are not driven by presynaptic action potentials, and the information transmitted per energy used drops off at low p values (red curves in Figure 3E), because the frequency of evoked release becomes comparable with that of spontaneous release. For a physiological spike rate (s = 0.01 per 2.5 ms interval, implying 4 Hz firing), and a total spontaneous release rate onto the cell of 1.2 Hz as measured in cortical pyramidal cells (Dani et al., 2005) so that m = 0.003 for a 2.5 ms interval, this creates an optimal release probability in the range 0.05–0.25, depending on the number of synapses converging onto the postsynaptic cell. Figure 3E (red lines) predicts that the optimal release probability is lower the more synapses that a single axon makes onto the same postsynaptic neuron. Strikingly, just such a relationship between release probability and number of release sites has been reported by Hardingham et al. (2010) (their Figure 7C) for cortical synapses and Branco et al. (2008) (their Figure 2D) for hippocampal synapses, with a mean release probability of ~0.7 at connections with a single release site declining to ~0.25–0.4 for connections with 4 release sites and to ~0.1 at connections with ~10 release sites. While there are some quantitative differences between their measurements and our Figure 3E (in particular their release probability being less than one for single release sites), this provides an important experimental confirmation of the unexpected inverse relationship between p and N that the analysis above predicts.

Thus, if axons make multiple synapses onto each postsynaptic cell (as is found experimentally)—perhaps in order to provide stable information processing in the face of spine turnover (Xu et al., 2007)—more information is transmitted per energy used by having a low release probability. (This conclusion, and all of the analysis in this section, is independent of the amount of ion entry generating a postsynaptic EPSC [provided this quantity is the same for all release sites] and so does not depend on exactly which receptor subunits are expressed at the synapses.) Consequently, although synaptic failures appear intuitively to be wasteful, they allow the energy use per bit of information transmitted to be minimized.

Another argument for having a low release probability to reduce energy use depends on the fact that a cortical neuron typically receives about 8,000 synapses on its dendritic tree (Braitenberg and Schüz, 1998). Levy and Baxter (2002) pointed out that the rate at which information arrives at all these synapses is greater than the rate at which the output axon of the cell can convey information, implying that energy is wasted on transmitting information that cannot possibly be passed on by the postsynaptic cell. They suggested that failures of synaptic transmission would reduce this energy waste. With the assumptions that all input synapses are independent and that their axons fire at the same energy-limited optimal rate (Equation 2) as does the postsynaptic cell's output axon, Levy and Baxter (2002) showed that the firing rate of the axons defines an optimal failure rate for synaptic transmission given by

$$
1-p = \left(\frac{1}{4}\right)^{I_{input}(s^*)}
\tag{6}
$$

where p is the synaptic release probability, I_{input} is defined by Equation 1, and $s*$ is the spike probability defined by Equation 2. Surprisingly, this ideal failure rate does not depend on the number of synaptic inputs to the cell (if there are more than a few hundred synapses). Figure 3F shows how Equation 6 predicts that the release probability should vary with the factor, r, by which energy consumption is increased during spiking. For the energy budget in Figure 2, $r = 150$ (see Figure 3F legend) and the predicted optimal release probability is approximately 0.2.

The Levy and Baxter (2002) analysis can be questioned. In general there will be multiple synapses from one axon onto the postsynaptic cell (see above) and it is unlikely that the action potential rate in the postsynaptic cell will be the same as in all of its afferents. Most importantly, most neurons do not exist simply to transmit all incoming information (e.g., a Purkinje cell does not pass on all the information arriving on its $\sim10^5$ parallel fiber inputs; instead, it makes a decision on how to modulate motor output based on those inputs). Nevertheless, Levy and Baxter's analysis provides another insight into how synaptic energy consumption implies that presynaptic terminals must be constrained to have a low release probability.

This analysis has focused on how presynaptic properties affect postsynaptic energy use, since it is postsynaptically that most energy is used (Figure 2). Nevertheless, energetic constraints on presynaptic function itself probably exist, e.g., there may be an optimal number of vesicles to have in a presynaptic terminal, to allow the maximal rate of information transmission that occurs through the synapse while minimizing energy costs on vesicle formation and trafficking.

Energy Use Limits the Number of Postsynaptic Receptors on Spines

How does energy use constrain postsynaptic properties? The energy budget of Figure 2 indicates that most energy use in the brain is on reversing the ion flux through postsynaptic receptors, which consumes 50% of the signaling energy use (or, including housekeeping energy use, 37% of all the energy the brain uses). On energetic grounds, therefore, fewer receptors per synapse would be better, since they will consume less energy. What is the optimal number of postsynaptic receptors to have at a synapse? For excitatory synapses to be able to repeatedly transmit information on a time scale of milliseconds, the diameter of synaptic boutons and spines must be less than ~1 μm, to allow rapid glutamate clearance by diffusion to glutamate transporters in surrounding astrocytes (Attwell and Gibb, 2005), and many spines are much smaller (Nusser et al., 1998). Does the small size of spines limit the number of receptors present, or are other factors relevant?

At different synapses, electrophysiology suggests that 10–70 AMPA receptors are opened by a single vesicle (Hestrin, 1992a; Silver et al., 1996; Spruston et al., 1995), while immunogold labels 8–40 postsynaptic AMPA receptors (Nusser et al., 1998). These numbers are underestimates, because the open probability of the receptors at the peak of the synaptic current is less than 1 (even in saturating glutamate) and because some receptors will not be labeled by immunocytochemistry. The probable true density is thus ~20–100 receptors per bouton.

For a postsynaptic area of 0.03 to 0.1 $(\mu m)^2$ (Momiyama et al., 2003; Nusser et al., 1998), 100 receptors would imply a density of 1,000–3,300 receptors $/(\mu m)^2$ to which NMDA and metabotropic receptors must also be added. This is comparable to the highest density of voltage-gated Na$^+$ channels achieved (at the node of Ranvier, 1300$/(\mu m)^2$: Hille, 2001), suggesting that spine size may constrain the number of channels present. However, spines vary extensively in size (Nusser et al., 1998), suggesting that more receptors could be added by expanding the postsynaptic area. The following analysis suggests that both energy use and postsynaptic noise, the effects of which on detection of vesicle release we have ignored above, are major determinants of the number of receptors present per spine.

We will consider two types of synapse—a "relay synapse," such as the optic tract to lateral geniculate nucleus synapse (the function of which is to simply pass on information), and an "information processing synapse" (signals at a large number of which sum to affect the output of the postsynaptic cell). For a relay synapse, if the number of receptors (and hence the synaptic current injected postsynaptically) is too small, then no postsynaptic action potential will be produced and none of the information arriving presynaptically will be transmitted (Figure 4A). Above the threshold for action potential production, if a postsynaptic action potential is reliably produced then all the arriving information is transmitted (although with large synaptic currents more than one postsynaptic action potential may occur and information could be degraded). The ratio of information transmitted to energy used postsynaptically (proportional to postsynaptic charge entry) will thus be as in Figure 4B, with an optimum at a value for the number of postsynaptic receptors that just produces an action potential. To produce a more reliable relay synapse, the safety factor could be improved with only a minor decrease in the ratio of information passed to energy used, by increasing the number of receptors slightly to ensure that postsynaptic voltage noise does not prevent an action potential being produced. However, large increases in the number of receptors per synapse merely decrease energy efficiency without affecting information transfer (Figure 4B).

For an information processing synapse, we consider the simple computation where a neuron has to produce an action potential if more than N synapses are activated. Suppose that each excitatory input synapse has K postsynaptic receptors of conductance $g_{channel}$ and reversal potential V_{syn}, which open with probability $p_{channel}$ when a vesicle is released. When N synapses are activated the mean synaptic conductance will be $G_{syn} = N \cdot K \cdot p_{channel} \cdot g_{channel}$ and for a cell of resting conductance G_{rp} at a resting potential V_{rp} the depolarization produced (ignoring the membrane capacitance for simplicity) will be

$$\Delta V = \frac{G_{syn} \cdot (V_{syn} - V_{rp})}{(G_{syn} + G_{rp})}$$

If this is to reach the threshold depolarization for producing an action potential, ΔV_{thresh}, then the synaptic conductance must satisfy

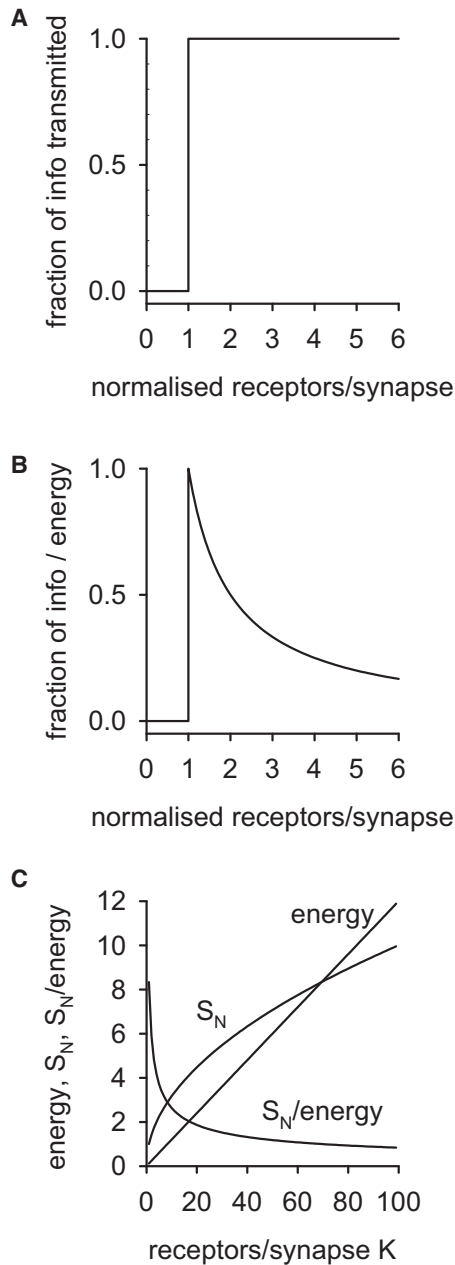$$G_{syn} = \frac{G_{rp}}{[(V_{syn} - V_{rp})/\Delta V_{thresh} - 1]},$$

Figure 4. Energy limitations on number of postsynaptic receptors.
(A) Schematic dependence of the fraction of information transmitted by a relay synapse on the number of postsynaptic receptors per synapse (normalized to the number needed to generate an action potential). Below the threshold for action potential production no information is transmitted; above the threshold transmission is reliable.
(B) Ratio of fraction of information transmitted to energy used postsynaptically for the synapse of (A). Energy used is proportional to the number of receptors activated. Increasing the receptor number above the value needed to ensure transmission decreases the energy efficiency of the synapse. In practice the sharpness of the optimum in (B) will be degraded by noise.
(C) Dependence on the number of receptors in a postsynaptic spine, K, of the energy used on postsynaptic current (arbitrary units), the signal to noise ratio of the current (S_N), and the signal-to-noise ratio to energy use (arbitrary units). The open probability of each activated receptor was assumed to be 0.5.

so that the number of postsynaptic receptors needed is

$$K = \frac{G_{rp}}{\left\{ N \cdot p_{channel} \cdot g_{channel} \cdot \left[\left(V_{syn} - V_{rp} \right) \big/ \Delta V_{thresh} - 1 \right] \right\}}. \quad (7)$$

The postsynaptic energy use will depend on the total number of synapses impinging on the cell and their rates of activation, but will be proportional to K. Equation 7 shows that this energy expenditure is proportional to the resting conductance of the cell, G_{rp}. The energy used on reversing Na^+ entry at the resting potential is also proportional to G_{rp} (Attwell and Laughlin, 2001). Why not, therefore, reduce the cell's resting conductance, to reduce proportionally the energy used both on postsynaptic currents and on the resting potential?

Although some cells have evolved to be extremely tiny and with a high resistance (e.g., cerebellar granule cells), there are two limitations to the miniaturization and energy saving that can be achieved in this way. First, as the number of receptors at each synapse is decreased, fluctuations in the number which are opened when a vesicle is released contribute increasingly significant variability to the synaptic current, because the receptor channel open probability (even for a saturating glutamate concentration) is not 1 but is ∼0.5–0.8 (Hestrin, 1992a; Spruston et al., 1995; Silver et al., 1996; Momiyama et al., 2003). For a single synapse, the signal-to-noise ratio (the ratio of the mean current produced by a vesicle to the standard deviation of that current) is related to the number of receptors (K) and their open probability ($p_{channel}$) by $\sqrt{(K \cdot p_{channel}/(1-p_{channel}))}$. Reducing K from 50 to 5 channels with $p_{channel} = 0.5$ would reduce the signal to noise ratio from 7.1 to 2.2 (Figure 4C). Nevertheless, because synaptic energy use is proportional to K, the signal-to-noise ratio achieved per energy used increases as K is decreased (Figure 4C). Thus, one can question what sets the lowest value of K that evolution has produced. One answer is that the synaptic signal must not fall below the size of the voltage noise generated by other ion channels in the neuron. The second limit to miniaturization is that, when the resistance of the cell is increased excessively, spontaneous opening of ion channels can trigger unwanted action potentials (Faisal et al., 2005). For example, the adult cerebellar granule cell membrane resistance is ∼1 GΩ (Cathala et al., 2003) so that, from Equation 7 (with $p_{channel} = 0.7$ [Momiyama et al., 2003], $g_{channel} = 12$ pS [Silver et al., 1996], $V_{syn} = 0$mV, $V_{rp} = -60$mV, and $\Delta V_{thresh} = 30$mV), $K = 120$, 60, 30, or 15 postsynaptic channels are needed if simultaneous activity in $N = 1$, 2, 3 or all (respectively) of the cell's four input synapses should evoke an action potential (experimentally the number of receptors present is 24–170 [Silver et al., 1996], consistent with these estimates). If the resistance were increased 20-fold, to reduce by a factor of 20 the energy used on postsynaptic currents and on the resting potential, then opening of a single 50 pS NMDA receptor by a stray glutamate molecule would depolarize the cell by 30mV and evoke an action potential.

In the above analysis we have considered pre- and postsynaptic constraints on energy use separately. This is valid because the effects on postsynaptic energy use of release probability and of the number of postsynaptic receptors are purely multiplicative, so the number of postsynaptic receptors does not affect

the optimal release probability in Figure 3E, and reducing the number of postsynaptic receptors will reduce energy use independent of the value of *p*. Thus, both energy minimization approaches are expected to be used physiologically.

Synapse Energy Is Mainly Provided by Mitochondria

The previous sections assessed how synapse properties can maximize the information that synapses transmit while reducing the energy used. But how is the massive energy use of synapses sustained? Averaged over time, in the adult brain ATP is almost entirely generated by the complete oxidation of glucose. Glycolysis followed by oxidative phosphorylation results in a ratio of oxygen to glucose consumption of nearly 6:1, and mitochondria (using the citric acid cycle followed by oxidative phosphorylation) provide ∼93% of the ATP generated (Sokoloff, 1960), with only ∼7% coming from glycolysis. Consistent with this, mitochondria are preferentially localized to pre- and postsynaptic sites where ATP is consumed (Wong-Riley, 1989; Chang et al., 2006). Nevertheless, when neuronal activity increases during perceptual tasks like those used in functional imaging experiments, which increase energy consumption by only a small percentage (Schölvinck et al., 2008; Lin et al., 2010), it has been suggested that ATP might be generated preferentially by glycolysis.

This idea arose because glycolytic enzymes can be closely associated with the sodium pump and may thus provide it with ATP in a spatially localized compartment (Knull, 1978; Lipton and Robacker, 1983). Furthermore, the increase in O_2 uptake during a perceptual task was found to be small compared to the increase in glucose uptake, suggesting that glycolytic ATP generation dominates (Fox et al., 1988), although Madsen et al. (1999) found less discrepancy between the increase of glucose and of O_2 use. However, neuronal activity evokes a decrease in extracellular O_2 (Malonek and Grinvald, 1996; Thompson et al., 2003) and intracellular NADH (Kasischke et al., 2004; Brennan et al., 2006) concentrations, implying that ATP is being generated by oxidative phosphorylation, and recent quantitative work has shown that most ATP produced in response to increases of neuronal activity is generated by mitochondria (Lin et al., 2010; Hall et al., 2012). So far there is no evidence to support the idea that pre- and postsynaptic terminals rely to a different extent on glycolysis and mitochondria for their ATP supply: both consume O_2 when neuronal activity is increased (Hall et al., 2012).

Astrocytes May Channel Energetic Substrates to Synaptic Mitochondria

How do the metabolic substrate(s) needed for ATP production flow to synaptic mitochondria? A simple assumption would be that pyruvate is provided to the mitochondria by glycolysis within the neuron. However, the morphology of astrocytes, with an extensive endfoot around blood vessels, is well suited to taking up glucose arriving in the blood and distributing it, or pyruvate or lactate derived from it, to astrocytic processes surrounding synapses, possibly after diffusion through gap junctions coupling adjacent astrocytes (Rouach et al., 2008). Furthermore, while most brain energy is used by synapses, the brain's only energy store, glycogen, which can sustain neuronal function

for a few minutes when the glucose and oxygen supply is compromised (Allen et al., 2005), is located in astrocytes (Gruetter, 2003), again suggesting metabolite transfer from astrocytes to neurons.

Pellerin and Magistretti (1994) proposed an astrocyte-neuron lactate shuttle, whereby (mainly glycolytic) astrocytes generate lactate, and export it to (mainly oxidative) neurons where it would be converted to pyruvate for ATP generation in mitochondria. Elegantly, such a scheme could regulate the energy supplied to neurons in response to their activity, since glutamate released by active neurons could promote lactate production in astrocytes by stimulating glycolytic ATP generation to power astrocytic uptake of glutamate and its conversion to glutamine. Neuronal activity does elevate lactate levels in the brain (Prichard et al., 1991), some studies (but not others) show that lactate can replace glucose as a power source for neurons (Schurr et al., 1988; Allen et al., 2005; Wyss et al., 2011), and lactate transporters are found in postsynaptic spines where most neuronal ATP is used (Bergersen et al., 2005). However, the extent to which astrocytes "feed" neurons, and even the direction of any lactate flux between the two cell types, remain controversial (Jolivet et al., 2010; Mangia et al., 2011). Consequently, a demonstration that long-term potentiation and memory are disrupted by deletion of lactate transporters (Suzuki et al., 2011; Newman et al., 2011) might reflect a signaling role for lactate, rather than an energetic one. Indeed, one way in which lactate may provide synapses with energy is by being employed as a prostaglandin-modulating messenger to increase blood flow (Gordon et al., 2008; Attwell et al., 2010).

Increasing the ATP Supply from Synaptic Mitochondria

Synaptic activity is far from constant and changes dramatically on time scales from seconds to days. How then is ATP production by synaptic mitochondria regulated to match this demand? We will consider short-term regulation of energy supply in this section, and long-term regulation below.

When ATP is consumed pre- and postsynaptically by the processes shown in Figure 1, the resulting increase of [ADP]/[ATP] will, by the law of mass action, tend to increase ATP formation by oxidative phosphorylation (Chance and Williams, 1955). However, the rise of $[Ca^{2+}]_i$ that occurs presynaptically to control transmitter release and postsynaptically at synapses expressing NMDA receptors (or Ca^{2+}-permeable AMPA receptors) provides another stimulus increasing ATP production rapidly in response to synaptic activity (Chouhan et al., 2012; see Gellerich et al. [2010] for a review and Mathiesen et al. [2011] for an opposing view). The rise of $[Ca^{2+}]_i$ leads to a rise of mitochondrial $[Ca^{2+}]_i$, which activates mitochondrial dehydrogenases that promote citric acid cycle activity (Duchen, 1992). The rise of cytoplasmic $[Ca^{2+}]_i$ also activates the mitochondrial aspartate-glutamate exchanger aralar (Gellerich et al., 2009), which raises [NADH] in mitochondria and thus supports H^+ pumping out across the mitochondrial membrane and subsequent ATP synthesis. Antiapoptotic Bcl2 family proteins may also regulate ATP production by decreasing ion leak through the F_1F_O ATP synthase (Alavian et al., 2011).

Activity-evoked entry of Ca^{2+} into synaptic mitochondria buffers the cytoplasmic $[Ca^{2+}]_i$ rise occurring (Billups and
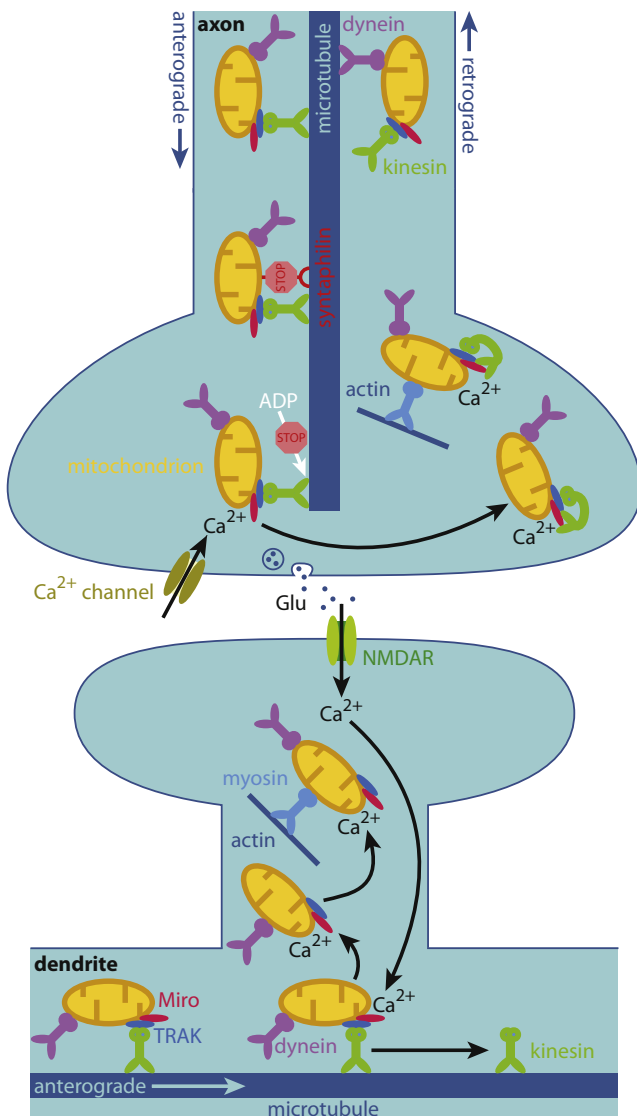
Figure 5. Trafficking of Mitochondria to Synapses
Mitochondria move long distances along microtubules, driven by kinesin and dynein motors, and shorter distances along actin filaments, driven by myosin motors. Conversion of ATP to ADP by ATPases like the Na$^+$ pump reduces the energy available for motor-driven transport, and ADP rebinding to the motor slows its movement. Calcium entering through presynaptic voltage-gated channels or postsynaptic NMDA receptors (or perhaps Ca^{2+}-permeable AMPA/kainate receptors) binds to the adaptor protein Miro and stops kinesin motors moving the mitochondrion. Contrasting models for how this occurs are drawn pre- and postsynaptically. Once stopped, mitochondria may be tethered to microtubules by syntaphilin.

Forsythe, 2002). Presynaptically this may, as well as altering energy supply, modulate synaptic release probability and its short-term plasticity. Postsynaptically it may reduce signaling (including synaptic plasticity) mediated by synaptically evoked elevations of [Ca^{2+}]$_i$. These actions will also impact on energy consumption: presynaptic mitochondrial Ca^{2+} buffering may reduce release probability to be in a region where the information transmitted per energy used is maximized (Figure 3). Similarly,

postsynaptic mitochondria, by buffering Ca^{2+} and reducing AMPA receptor insertion into the membrane (see below), may reduce postsynaptic energy expenditure.

Synaptic activity can also decrease mitochondrial activity. Endocannabinoids released by synapses have been suggested to suppress presynaptic mitochondrial respiration (Bénard et al., 2012). This contributes to depolarization-induced suppression of inhibition— short-term plasticity in which postsynaptic depolarization reduces presynaptic GABA release.

Locating Mitochondria at Synapses
In addition to short term regulation of the ATP output of individual mitochondria, the preferential positioning of mitochondria at pre- and postsynaptic terminals (Chang et al., 2006) is of key importance in the long-term regulation of power to synapses. Presynaptic terminals in neocortex contain between 0.3 and 1.4 mitochondria (Sakata and Jones, 2003), while postsynaptically in cultured hippocampal neurons there is ~1 mitochondrion per 7 μm of dendrite, which is comparable to the 6 μm separation of synapses (MacAskill et al., 2009). Thus, on either side of most synapses there is ~1 mitochondrion.

Mitchondria are formed at the soma. ATP synthesized here would take over 2 min to diffuse to the end of a 200-μm-long dendrite, and ~10 years to diffuse to the end of a 1-m-long axon, preventing rapid adaptation of the ATP supply in response to changing pre- and postsynaptic activity. Instead, therefore, mitochondria are transported long distances around neurons by kinesin and dynein motors, moving on microtubule tracks at ~0.3–1 μm/s. This has been reviewed extensively by MacAskill et al. (2010) and Sheng and Cai (2012), who provide more detail on the following points. In the axon, kinesin motors (mainly KIF5) move mitochondria away from the soma, while dynein mainly moves mitochondria toward the soma, but in dendrites (where the microtubule polarity is mixed) both motors can operate in either direction (Figure 5). More local movements of mitochondria are mediated by myosin V (plus-end directed), VI (minus-end directed), and perhaps XIX motors operating on actin tracks (Ligon and Steward, 2000), and myosin activity also opposes mitochondrial motion along microtubules (Pathak et al., 2010). Since microtubules may not often enter dendritic spines (Conde and Cáceres, 2009), actin-based movement may be needed to make mitochondria protrude into the spines (Li et al., 2004). At any one time a majority (~80%) of mitochondria are stationary. What determines where mitochondria get "parked," so they are able to function as a local power source or calcium buffer?

Figure 5 summarizes our understanding of how mitochondria move around neurons, and the mechanisms by which they are positioned at pre- and postsynaptic sites. For the various cellular motors to transport mitochondria, they need to consume ATP, and the motors need to be attached to the mitochondria via adaptor molecules (Milton/TRAK, Miro, and Syntabulin). Regulation of mitochondrial movement occurs both at the level of motor function, through local alterations of ADP/ATP ratio, and at the level of the attachment of mitochondria to the motors and the tracks they move along, through local changes in [Ca^{2+}]$_i$ (Brough et al., 2005; Mironov, 2006).

Postsynaptically, increased energy expenditure on glutamate-induced ion fluxes leads to a local rise in [ADP] and a fall of [ATP].

This decreases the energy available to the motor molecules transporting mitochondria, and rebinding of ADP to the motors in particular slows their movement (Mironov, 2007). A similar phenomenon occurs in axons in response to ATP use on pumping out of Na^+ at the Ranvier node (Zhang et al., 2010) and so is also expected during energy use on Ca^{2+} pumping and vesicle trafficking in presynaptic terminals (Figure 5).

In addition to this energetic limitation of mitochondrial movement, the rise in $[Ca^{2+}]_i$ that occurs presynaptically via voltage-gated Ca^{2+} channels, and postsynaptically via Ca^{2+} influx through NMDA receptors (and possibly Ca^{2+}-permeable AMPA/kainate receptors), leads to a parking of mitochondria at the active synapse. Wang and Schwarz (2009) found that a rise in axonal $[Ca^{2+}]_i$ in hippocampal neurons leads to mitochondrial stopping, following Ca^{2+} binding to the adaptor protein Miro, which resulted in kinesin motors detaching from their microtubule tracks (Figure 5, presynaptic side; Ca^{2+} entry into the mitochondria may be needed for this to occur: Chang et al., 2011). A similar arrest of mitochondrial movement in dendrites is triggered by Ca^{2+} entering through postsynaptic NMDA receptors (Rintoul et al., 2003; MacAskill et al., 2009). In this case the proposed mechanism differed: Ca^{2+} binding to Miro was suggested to detach Miro from the kinesin motor (Figure 5, postsynaptic side). Calcium may also regulate mitochondrial transport by myosin, since Ca^{2+} stimulates myosin-actin ATPase activity but also (presumably at higher $[Ca^{2+}]_i$) decreases transport by dissociating calmodulin from myosin (Lu et al., 2006; Taylor, 2007). Speculatively, therefore, a small $[Ca^{2+}]_i$ rise may stop microtubule-based transport (MacAskill et al., 2009; Wang and Schwarz, 2009) and promote local actin-based transport, until the mitochondrion encounters a higher $[Ca^{2+}]_i$, which will stop actin-based transport. At present little is known about the localization of mitochondria at the postsynaptic side of inhibitory synapses where no local rise of $[Ca^{2+}]_i$ is expected: in the mature animal the chloride reversal potential is close to the resting potential so restoring postsynaptic Cl^- gradients uses less energy than for Na^+ gradients (Howarth et al., 2010) and a concentration of mitochondria at this site may not be needed.

Brief synaptic calcium entry (for ~1 s) evokes a cessation of long-range mitochondrial movement for about 3 min (MacAskill et al., 2009), which presumably reflects the time needed for Miro to release its bound Ca^{2+} and for a functioning mitochondrion-adaptor-kinesin complex to reform. However mitochondria are often immobile for periods longer than this. In axons and presynaptic terminals this can reflect tethering to microtubules by syntaphilin (Kang et al., 2008) aided by the dynein light chain LC8 (Chen et al., 2009), while prolonged protrusion of mitochondria into dendritic spines (Li et al., 2004) may reflect a similar tethering to actin filaments. In some presynaptic terminals, anatomical specializations may also help to localize mitochondria near synaptic vesicle pools (Wimmer et al., 2006).

The localization of mitochondria, both pre- and postsynaptically, produced by [ADP] and $[Ca^{2+}]_i$ rises, and by tethering molecules, is crucial for neuronal function. In *Drosophila*, presynaptic motor neuron terminals lacking functional mitochondria (because of Miro mutations that prevent kinesin-based transport) cannot sustain vesicle release during prolonged activity (Guo et al., 2005), because of a failure of myosin-driven mobilisa-

tion of reserve pool vesicles (Verstreken et al., 2005). A similar phenomenon is seen in mammalian neurons in which the level of another adaptor linking mitochondria to kinesin motors, syntabulin, is reduced (Ma et al., 2009). In hippocampal neurons, tethering by syntaphilin of axonal mitochondria increases presynaptic Ca^{2+} buffering and thus decreases short-term facilitation of synaptic transmission (Kang et al., 2008), while in the crayfish neuromuscular junction and the mammalian calyx of Held presynaptic mitochondrial Ca^{2+} buffering promotes synaptic transmission after a train of impulses (Tang and Zucker, 1997; Billups and Forsythe, 2002). Postsynaptically, during synaptogenesis, mitochondria move into dendritic protrusions in response to synaptic excitation (Li et al., 2004). This was triggered by NMDA receptor activation, which has two effects: Miro-mediated halting of microtubule-based mitochondrial transport along the dendrite (MacAskill et al., 2009) followed by promotion of actin-based movement into the protrusion by the WAVE1 protein (Sung et al., 2008). This relocation correlated with the development of spines in that region, perhaps because ATP is needed for spine formation. A more extreme effect is provided by mutations of the protein sacsin that decrease mitochondrial potential and result in mitochondria being too large to enter small dendrites of cerebellar Purkinje cells. This causes Purkinje cell degeneration and consequent spastic ataxia (Girard et al., 2012). Thus, correct location of functioning mitochondria at synapses is important both for the development of the nervous system, and for its plasticity and health in the adult.

Developmental Changes in Synaptic Function and Energy Use

The preceding sections have explained how synapses can reduce their energy use and where they get their energy from. We turn now to changes of synaptic energy use in development, synaptic plasticity, and sleep.

As brains develop they initially increase their energy use above the adult value, but beyond adolescence aging is associated with a decrease of energy use (Gleason et al., 1989; Leenders et al., 1990). These changes correlate with an increase in the thickness of the cortex as many synaptic connections are made, followed by cortical thinning as connections are pruned and the brain reaches its mature state (reviewed by Harris et al., 2011). The high energy use during development reflects not only the larger number of energy-consuming synapses but also the ATP used to synthesize cellular components.

On top of changes in the number of synapses, changes in the energy used per synapse occur during development, as a result of the recruitment of AMPA receptors to excitatory synapses that initially contain mainly NMDA receptors (Hall and Ghosh, 2008), and changes in the NMDA receptor subunits present which shorten the synaptic current and thus reduce ATP consumption (Hestrin, 1992b). Furthermore, GABAergic synapses may use more energy early in development, when the accumulation of Cl^- by NKCC1 transporters results in $GABA_A$ receptors being excitatory, compared with the mature brain, when the $[Cl^-]$ gradient is set by KCC2 transporters exporting Cl^- and $GABA_A$ receptors are inhibitory (Ben-Ari, 2002). Early in development restoring the $[Cl^-]$ gradient, after synaptic transmission causes a depolarizing efflux of Cl^-, will

require Na$^+$ entry on NKCC1 (and hence subsequent ATP use on the Na$^+$ pump), unlike in the mature brain where reversing a hyperpolarizing Cl$^-$ influx is performed by KCC2 and uses little energy (Howarth et al., 2010).

Synaptic Plasticity and Energy Use

As in the developing brain, synaptic strength in the mature brain can be increased or decreased by plasticity processes, and this will alter energy expenditure. For example, NMDA receptor-dependent long-term potentiation can double the strength of synapses by inserting more AMPA receptors into the postsynaptic membrane, doubling their postsynaptic energy consumption and requiring an increased ATP supply to the potentiated synapses (Wieraszko, 1982). Accordingly, a negative feedback mechanism mediated by AMP-dependent protein kinase prevents the maintenance of synapse potentiation when cellular energy supplies are challenged (Potter et al., 2010). In addition, long-term potentiation and memory are disrupted by deletion of lactate transporters (Suzuki et al., 2011; Newman et al., 2011), but it is unclear whether this reflects an energetic or a signaling function of lactate (see above). To avoid a progressive increase in synapse strength and hence in energy expenditure, homeostatic plasticity renormalizes the strengths of synapses (Turrigiano, 2012), in part employing release of TNFα from astrocytes (Stellwagen and Malenka, 2006). This downward adjustment of synaptic currents occurs, at least partly, during sleep (see below).

Synaptic plasticity can also offer energetic savings to synaptic transmission. Long-term depression of the cerebellar parallel fiber to Purkinje cell synapse, used to learn motor patterns, ultimately results in ∼85% of the synapses producing no postsynaptic current (Isope and Barbour, 2002). The existence of silent synapses is predicted theoretically for optimal storage of information (Brunel et al., 2004) but also provides a massive decrease in the amount of energy used synaptically (Howarth et al., 2010).

Sleep and Synaptic Energy Use

Increasingly, sleep is thought to play an energetically restorative role in the brain (Scharf et al., 2008). This theory coincides with most people's experience of sleep but has found direct physiological support only recently. Dworak et al. (2010) reported that during sleep there is a transient increase in ATP level in cells of awake-active regions of the brain. This was suggested to fuel restorative biosynthetic processes in cells that, during the day, must use all of their energy on electrical and chemical signaling. This implies an energy consumption trade-off: a high use of ATP on synapses during awake periods is balanced by more ATP being allocated to other tasks during sleep.

Energy use in the awake state also increases due to synaptic potentiation. In the awake state (compared to sleep), GluR1 subunits of AMPA receptors are present at a higher level and in a more phosphorylated state (consistent with an increased synaptic strength), synaptic currents and spine numbers increase, and evoked neuronal responses are larger (Vyazovskiy et al., 2008; Maret et al., 2011). These changes are reversed during sleep, presumably because of homeostatic plasticity as discussed above. Thus, sleep is essential for adjusting synaptic energy use.

Disorders of Synapse Energetics

Finally, we turn to the pathological effects of disruptions to synaptic energetics. Since synapses account for the majority of energy use in the brain, any disorder of mitochondrial trafficking or function will inevitably affect synapses. Reciprocally, excessive glutamatergic synaptic transmission raises neuronal [Ca^{2+}]$_i$, which depolarizes mitochondria, reducing their ATP production and in extremis leading to cytochrome C release and the initiation of apoptosis. Increasingly, one or other of these mitochondrial dysfunctions is reported as contributing to brain disorders.

Mitochondrial dysfunction may contribute to neuronal damage in Parkinson's disease (Youle and Narendra, 2011). Dopaminergic neurons in the substantia nigra consume a significant amount of ATP to reverse the Ca^{2+} influx that mediates their pacemaking activity (Puopolo et al., 2007). Producing this ATP leads to oxidative stress (Guzman et al., 2010) that can uncouple or depolarize mitochondria. Such compromised mitochondria, which produce less ATP, must be replaced to allow the cell to continue functioning. The mechanism for this involves two proteins, PINK1 and Parkin (Geisler et al., 2010). The PINK1 level on the mitochondrial surface is enhanced by mitochondrial damage and depolarization, which leads to PINK1 recruiting the E3 ubiquitin ligase Parkin to initiate degradation of outer mitochondrial membrane proteins (Chan et al., 2011), including the mitochondrial fusion proteins mitofusin 1 and 2 and the transport adaptor protein Miro. Mitofusin degradation prevents damaged mitochondria from fusing with healthy mitochondria (Tanaka et al., 2010), while Miro degradation, which may occur after PINK1 phosphorylates Miro (Wang et al., 2011; but see Liu et al., 2012a), detaches the mitochondrion from its kinesin motor, anchoring it until it is eliminated by an autophagosome (Cai et al., 2012). When this pathway is deranged, as occurs with mutations in PINK1 or Parkin that give rise to hereditary forms of Parkinson's disease (Kitada et al., 1998; Valente et al., 2004), malfunctioning mitochondria will not provide sufficient ATP at synapses.

In Huntington's disease (HD), mitochondrial defects may contribute to the preferential loss of spiny GABAergic neurons in the striatum (Damiano et al., 2010). Expression of mutant huntingin (mhtt) disrupts trafficking of mitochondria to synapses before the onset of neurological symptoms and synaptic degeneration (Trushina et al., 2004) and leads to accumulation of fragmented mitochondria in the soma, as a result of altered activity of proteins mediating mitochondrial fission (Drp1) and fusion (Mfn1) (Kim et al., 2010; Shirendeb et al., 2012). This impaired trafficking of mitochondria may cause ATP deprivation at the synapse, eventually promoting synaptic degeneration. Disrupted mitochondrial Ca^{2+} buffering (Panov et al., 2002) may pose a further problem at synapses, making neurons more susceptible to excitotoxicity upon mhtt-enhanced or even normal activation of NMDA receptors (Fan and Raymond, 2007).

Mitochondrial abnormalities also occur in Alzheimer's disease (AD) (Maurer et al., 2000; Lin and Beal, 2006). Increased mitochondrial fission and decreased fusion occur, correlating with loss of dendritic spines (Wang et al., 2009), in part as a result of nitric oxide produced in response to the amyloid β (Aβ) that is a hallmark of AD (Cho et al., 2009). Mitochondrial damage by

Aβ results in oxidative stress, opening of the mitochondrial permeability transition pore and thus apoptosis (Sheehan et al., 1997; Du et al., 2008). Synaptic mitochondria are more sensitive to Aβ damage than nonsynaptic mitochondria: Aβ accumulation occurs earlier in synaptic than in nonsynaptic mitochondria, decreasing mitochondrial trafficking and respiratory function and increasing mitochondrial oxidative stress (Rui et al., 2006; Du et al., 2010). Tau, a microtubule associated protein that is hyperphosphorylated in AD and a major component of the neurofibrillary tangles that are the second hallmark of AD, is also implicated in mitochondrial disruption. Overexpression of tau, or expression of a mutated form mimicking hyperphosphorylated tau, inhibited mitochondrial movement in mouse cortical axons, perhaps by increasing microtubule spacing (Shahpasand et al., 2012), and so may disrupt the energy supply to synapses. Furthermore, abnormal tau can spread transsynaptically, propagating AD pathology and thus disrupting synaptic function throughout anatomically connected neurons (Liu et al., 2012b; de Calignon et al., 2012).

Mitochondrial abnormalities at the neuromuscular junction (NMJ) have been implicated in the rapidly fatal motor neuron disease, familial amyotrophic lateral sclerosis (FALS), 20% of which cases are caused by gain of function mutations in superoxide dismutase (SOD1). In SOD1-FALS, NMJs are the first regions of the motor neurons to degenerate (Frey et al., 2000; Fischer et al., 2004). Early abnormal mitochondrial accumulation at the NMJ suggests that impaired mitochondrial dynamics contribute to the disease (Vande Velde et al., 2004). However, experimental assessment of this idea has yielded conflicting results. Zhu and Sheng (2011) found that increasing mitochondrial mobility two-fold did not affect the onset of ALS-like symptoms. Magrané et al. (2012), on the other hand, found that neurons expressing mutant SOD1 had impaired mitochondrial fusion and transport toward the soma, associated with a reduced mitochondrial potential and mislocation at synapses. As a result there were abnormalities in synapse number, structure, and function.

Mitochondrial function is impaired in cerebral ischemia, when there is a cut-off of the normal supply of glucose and oxygen. Early in ischemia synaptic activity disappears (Hofmeijer and van Putten, 2012) when released adenosine blocks presynaptic Ca^{2+} influx and thus inhibits glutamate release (Fowler, 1990; Scholz and Miller, 1991). This early suppression of glutamate release may protect against glutamate excitotoxicity. However, if ischemia is prolonged, the rundown of ion gradients that results from inhibition of mitochondrial function leads to a reversal of glutamate transporters and a rise of extracellular glutamate concentration to ~200 μM (Rossi et al., 2000). This triggers a massive Ca^{2+} influx via NMDA receptors, and subsequent depolarization of mitochondria, release of cytochrome C, and neuronal apoptosis.

Conclusions

Of the brain's components, synapses consume most energy. Consequently, pre- and postsynaptic adaptations minimize synaptic energy use and maximize its supply. Surprisingly, the presence of more than one release site at synaptic connections implies that the information transmitted per ATP consumed can be maximized by employing release sites with a low release probability. Energy supply is maximized by mechanisms that increase mitochondrial ATP production in response to synaptic activity and target mitochondria to active synapses. Energy use may be distributed over awake and asleep states, with synaptic plasticity that increases ATP use concentrated during awake periods. Neurological disorders frequently involve deficits in synaptic energy supply. For the future, a better understanding of how ATP is supplied to synapses will be invaluable both in understanding information processing in the brain and in devising therapies for neurological disorders.

REFERENCES

Abeles, M. (1991). Corticonics: Neural Circuits of the Cerebral Cortex (Cambridge: CUP).

Aiello, L.C., and Wheeler, P. (1995). The expensive tissue hypothesis: the brain and the digestive system in human and primate evolution. Curr. Anthropol. *36*, 199–221.

Alavian, K.N., Li, H., Collis, L., Bonanni, L., Zeng, L., Sacchetti, S., Lazrove, E., Nabili, P., Flaherty, B., Graham, M., et al. (2011). Bcl-xL regulates metabolic efficiency of neurons through interaction with the mitochondrial F1FO ATP synthase. Nat. Cell Biol. *13*, 1224–1233.

Alle, H., Roth, A., and Geiger, J.R. (2009). Energy-efficient action potentials in hippocampal mossy fibres. Science *325*, 1405–1408.

Allen, N.J., Káradóttir, R., and Attwell, D. (2005). A preferential role for glycolysis in preventing the anoxic depolarization of rat hippocampal area CA1 pyramidal cells. J. Neurosci. *25*, 848–859.

Attwell, D., and Gibb, A. (2005). Neuroenergetics and the kinetic design of excitatory synapses. Nat. Rev. Neurosci. *6*, 841–849.

Attwell, D., and Laughlin, S.B. (2001). An energy budget for signaling in the grey matter of the brain. J. Cereb. Blood Flow Metab. *21*, 1133–1145.

Attwell, D., Buchan, A.M., Charpak, S., Lauritzen, M., Macvicar, B.A., and Newman, E.A. (2010). Glial and neuronal control of brain blood flow. Nature *468*, 232–243.

Balasubramanian, V., Kimber, D., and Berry, M.J., 2nd. (2001). Metabolically efficient information processing. Neural Comput. *13*, 799–815.

Ben-Ari, Y. (2002). Excitatory actions of gaba during development: the nature of the nurture. Nat. Rev. Neurosci. *3*, 728–739.

Bénard, G., Massa, F., Puente, N., Lourenço, J., Bellocchio, L., Soria-Gómez, E., Matias, I., Delamarre, A., Metna-Laurent, M., Cannich, A., et al. (2012). Mitochondrial CB₁ receptors regulate neuronal energy metabolism. Nat. Neurosci. *15*, 558–564.

Bergersen, L.H., Magistretti, P.J., and Pellerin, L. (2005). Selective postsynaptic co-localization of MCT2 with AMPA receptor GluR2/3 subunits at excitatory synapses exhibiting AMPA receptor trafficking. Cereb. Cortex *15*, 361–370.

Billups, B., and Forsythe, I.D. (2002). Presynaptic mitochondrial calcium sequestration influences transmission at mammalian central synapses. J. Neurosci. *22*, 5840–5847.

Braitenberg, V., and Schüz, A. (1998). Cortex: Statistics and Geometry of Neuronal Connectivity, Second Edition (Berlin: Springer).

Branco, T., Staras, K., Darcy, K.J., and Goda, Y. (2008). Local dendritic activity sets release probability at hippocampal synapses. Neuron 59, 475–485.

Brennan, A.M., Connor, J.A., and Shuttleworth, C.W. (2006). NAD(P)H fluorescence transients after synaptic activity in brain slices: predominant role of mitochondrial function. J. Cereb. Blood Flow Metab. 26, 1389–1406.

Brough, D., Schell, M.J., and Irvine, R.F. (2005). Agonist-induced regulation of mitochondrial and endoplasmic reticulum motility. Biochem. J. 392, 291–297.

Brunel, N., Hakim, V., Isope, P., Nadal, J.P., and Barbour, B. (2004). Optimal information storage and the distribution of synaptic weights: perceptron versus Purkinje cell. Neuron 43, 745–757.

Cai, Q., Zakaria, H.M., Simone, A., and Sheng, Z.H. (2012). Spatial parkin translocation and degradation of damaged mitochondria via mitophagy in live cortical neurons. Curr. Biol. 22, 545–552.

Carter, B.C., and Bean, B.P. (2009). Sodium entry during action potentials of mammalian neurons: incomplete inactivation and reduced metabolic efficiency in fast-spiking neurons. Neuron 64, 898–909.

Cathala, L., Brickley, S., Cull-Candy, S., and Farrant, M. (2003). Maturation of EPSCs and intrinsic membrane properties enhances precision at a cerebellar synapse. J. Neurosci. 23, 6074–6085.

Chan, N.C., Salazar, A.M., Pham, A.H., Sweredoski, M.J., Kolawa, N.J., Graham, R.L., Hess, S., and Chan, D.C. (2011). Broad activation of the ubiquitin-proteasome system by Parkin is critical for mitophagy. Hum. Mol. Genet. 20, 1726–1737.

Chance, B., and Williams, G.R. (1955). Respiratory enzymes in oxidative phosphorylation. III. The steady state. J. Biol. Chem. 217, 409–427.

Chang, D.T., Honick, A.S., and Reynolds, I.J. (2006). Mitochondrial trafficking to synapses in cultured primary cortical neurons. J. Neurosci. 26, 7035–7045.

Chang, K.T., Niescier, R.F., and Min, K.-T. (2011). Mitochondrial matrix Ca^{2+} as an intrinsic signal regulating mitochondrial motility in axons. Proc. Natl. Acad. Sci. USA 108, 15456–15461.

Chen, Y.M., Gerwin, C., and Sheng, Z.H. (2009). Dynein light chain LC8 regulates syntaphilin-mediated mitochondrial docking in axons. J. Neurosci. 29, 9429–9438.

Cho, D.H., Nakamura, T., Fang, J., Cieplak, P., Godzik, A., Gu, Z., and Lipton, S.A. (2009). S-nitrosylation of Drp1 mediates beta-amyloid-related mitochondrial fission and neuronal injury. Science 324, 102–105.

Chouhan, A.K., Ivannikov, M.V., Lu, Z., Sugimori, M., Llinas, R.R., and Macleod, G.T. (2012). Cytosolic calcium coordinates mitochondrial energy metabolism with presynaptic activity. J. Neurosci. 32, 1233–1243.

Chvátal, A., Anderová, M., Hock, M., Prajerová, I., Neprasová, H., Chvátal, V., Kirchhoff, F., and Syková, E. (2007). Three-dimensional confocal morphometry reveals structural changes in astrocyte morphology in situ. J. Neurosci. Res. 85, 260–271.

Conde, C., and Cáceres, A. (2009). Microtubule assembly, organization and dynamics in axons and dendrites. Nat. Rev. Neurosci. 10, 319–332.

Damiano, M., Galvan, L., Déglon, N., and Brouillet, E. (2010). Mitochondria in Huntington's disease. Biochim. Biophys. Acta 1802, 52–61.

Dani, V.S., Chang, Q., Maffei, A., Turrigiano, G.G., Jaenisch, R., and Nelson, S.B. (2005). Reduced cortical activity due to a shift in the balance between excitation and inhibition in a mouse model of Rett syndrome. Proc. Natl. Acad. Sci. USA 102, 12560–12565.

Dayan, P., and Abbott, L. (2001). Theoretical Neuroscience (Cambridge, MA: MIT Press).

de Calignon, A., Polydoro, M., Suárez-Calvet, M., William, C., Adamowicz, D.H., Kopeikina, K.J., Pitstick, R., Sahara, N., Ashe, K.H., Carlson, G.A., et al. (2012). Propagation of tau pathology in a model of early Alzheimer's disease. Neuron 73, 685–697.

de Ruyter van Steveninck, R.R., and Laughlin, S.B. (1996). The rate of information transfer at graded-potential synapses. Nature 379, 642–645.

Deuchars, J., and Thomson, A.M. (1995). Innervation of burst firing spiny interneurons by pyramidal cells in deep layers of rat somatomotor cortex: paired intracellular recordings with biocytin filling. Neuroscience 69, 739–755.

Du, H., Guo, L., Fang, F., Chen, D., Sosunov, A.A., McKhann, G.M., Yan, Y., Wang, C., Zhang, H., Molkentin, J.D., et al. (2008). Cyclophilin D deficiency attenuates mitochondrial and neuronal perturbation and ameliorates learning and memory in Alzheimer's disease. Nat. Med. 14, 1097–1105.

Du, H., Guo, L., Yan, S., Sosunov, A.A., McKhann, G.M., and Yan, S.S. (2010). Early deficits in synaptic mitochondria in an Alzheimer's disease mouse model. Proc. Natl. Acad. Sci. USA 107, 18670–18675.

Duchen, M.R. (1992). $Ca^{(2+)}$-dependent changes in the mitochondrial energetics in single dissociated mouse sensory neurons. Biochem. J. 283, 41–50.

Dworak, M., McCarley, R.W., Kim, T., Kalinchuk, A.V., and Basheer, R. (2010). Sleep and brain energy levels: ATP changes during sleep. J. Neurosci. 30, 9007–9016.

Faisal, A.A., White, J.A., and Laughlin, S.B. (2005). Ion-channel noise places limits on the miniaturization of the brain's wiring. Curr. Biol. 15, 1143–1149.

Fan, M.M., and Raymond, L.A. (2007). N-methyl-D-aspartate (NMDA) receptor function and excitotoxicity in Huntington's disease. Prog. Neurobiol. 81, 272–293.

Fischer, L.R., Culver, D.G., Tennant, P., Davis, A.A., Wang, M., Castellano-Sanchez, A., Khan, J., Polak, M.A., and Glass, J.D. (2004). Amyotrophic lateral sclerosis is a distal axonopathy: evidence in mice and man. Exp. Neurol. 185, 232–240.

Fowler, J.C. (1990). Adenosine antagonists alter the synaptic response to in vitro ischemia in the rat hippocampus. Brain Res. 509, 331–334.

Fox, P.T., Raichle, M.E., Mintun, M.A., and Dence, C. (1988). Nonoxidative glucose consumption during focal physiologic neural activity. Science 241, 462–464.

Frey, D., Schneider, C., Xu, L., Borg, J., Spooren, W., and Caroni, P. (2000). Early and selective loss of neuromuscular synapse subtypes with low sprouting competence in motoneuron diseases. J. Neurosci. 20, 2534–2542.

Geisler, S., Holmström, K.M., Skujat, D., Fiesel, F.C., Rothfuss, O.C., Kahle, P.J., and Springer, W. (2010). PINK1/Parkin-mediated mitophagy is dependent on VDAC1 and p62/SQSTM1. Nat. Cell Biol. 12, 119–131.

Gellerich, F.N., Gizatullina, Z., Arandarcikaite, O., Jerzembek, D., Vielhaber, S., Seppet, E., and Striggow, F. (2009). Extramitochondrial Ca^{2+} in the nanomolar range regulates glutamate-dependent oxidative phosphorylation on demand. PLoS ONE 4, e8181.

Gellerich, F.N., Gizatullina, Z., Trumbeckaite, S., Nguyen, H.P., Pallas, T., Arandarcikaite, O., Vielhaber, S., Seppet, E., and Striggow, F. (2010). The regulation of OXPHOS by extramitochondrial calcium. Biochim. Biophys. Acta 1797, 1018–1027.

Girard, M., Larivière, R., Parfitt, D.A., Deane, E.C., Gaudet, R., Nossova, N., Blondeau, F., Prenosil, G., Vermeulen, E.G., Duchen, M.R., et al. (2012). Mitochondrial dysfunction and Purkinje cell loss in autosomal recessive spastic ataxia of Charlevoix-Saguenay (ARSACS). Proc. Natl. Acad. Sci. USA 109, 1661–1666.

Gleason, C.A., Hamm, C., and Jones, M.D., Jr. (1989). Cerebral blood flow, oxygenation, and carbohydrate metabolism in immature fetal sheep in utero. Am. J. Physiol. 256, R1264–R1268.

Goldman, M.S. (2004). Enhancement of information transmission efficiency by synaptic failures. Neural Comput. 16, 1137–1162.

Gordon, G.R., Choi, H.B., Rungta, R.L., Ellis-Davies, G.C., and MacVicar, B.A. (2008). Brain metabolism dictates the polarity of astrocyte control over arterioles. Nature 456, 745–749.

Gruetter, R. (2003). Glycogen: the forgotten cerebral energy store. J. Neurosci. Res. 74, 179–183.

Guo, X., Macleod, G.T., Wellington, A., Hu, F., Panchumarthi, S., Schoenfield, M., Marin, L., Charlton, M.P., Atwood, H.L., and Zinsmaier, K.E. (2005). The GTPase dMiro is required for axonal transport of mitochondria to Drosophila synapses. Neuron 47, 379–393.

Guzman, J.N., Sanchez-Padilla, J., Wokosin, D., Kondapalli, J., Ilijic, E., Schumacker, P.T., and Surmeier, D.J. (2010). Oxidant stress evoked by pacemaking in dopaminergic neurons is attenuated by DJ-1. Nature *468*, 696–700.

Hall, B.J., and Ghosh, A. (2008). Regulation of AMPA receptor recruitment at developing synapses. Trends Neurosci. *31*, 82–89.

Hall, C.N., Klein-Flügge, M.C., Howarth, C., and Attwell, D. (2012). Oxidative phosphorylation, not glycolysis, powers presynaptic and postsynaptic mechanisms underlying brain information processing. J. Neurosci. *32*, 8940–8951.

Hardingham, N.R., Read, J.C.A., Trevelyan, A.J., Nelson, J.C., Jack, J.J.B., and Bannister, N.J. (2010). Quantal analysis reveals a functional correlation between presynaptic and postsynaptic efficacy in excitatory connections from rat neocortex. J. Neurosci. *30*, 1441–1451.

Harris, J.J., and Attwell, D. (2012). The energetics of CNS white matter. J. Neurosci. *32*, 356–371.

Harris, J.J., Reynell, C., and Attwell, D. (2011). The physiology of developmental changes in BOLD functional imaging signals. Dev. Cogn. Neurosci. *1*, 199–216.

Hestrin, S. (1992a). Activation and desensitization of glutamate-activated channels mediating fast excitatory synaptic currents in the visual cortex. Neuron *9*, 991–999.

Hestrin, S. (1992b). Developmental regulation of NMDA receptor-mediated synaptic currents at a central synapse. Nature *357*, 686–689.

Hille, B. (2001). Ion Channels of Excitable Membranes, Third Edition (Sunderland, MA: Sinauer).

Hofmeijer, J., and van Putten, M.J. (2012). Ischemic cerebral damage: an appraisal of synaptic failure. Stroke *43*, 607–615.

Howarth, C., Peppiatt-Wildman, C.M., and Attwell, D. (2010). The energy use associated with neural computation in the cerebellum. J. Cereb. Blood Flow Metab. *30*, 403–414.

Isope, P., and Barbour, B. (2002). Properties of unitary granule cell—>Purkinje cell synapses in adult rat cerebellar slices. J. Neurosci. *22*, 9668–9678.

Jolivet, R., Allaman, I., Pellerin, L., Magistretti, P.J., and Weber, B. (2010). Comment on recent modeling studies of astrocyte-neuron metabolic interactions. J. Cereb. Blood Flow Metab. *30*, 1982–1986.

Kang, J.S., Tian, J.H., Pan, P.Y., Zald, P., Li, C., Deng, C., and Sheng, Z.H. (2008). Docking of axonal mitochondria by syntaphilin controls their mobility and affects short-term facilitation. Cell *132*, 137–148.

Kasischke, K.A., Vishwasrao, H.D., Fisher, P.J., Zipfel, W.R., and Webb, W.W. (2004). Neural activity triggers neuronal oxidative metabolism followed by astrocytic glycolysis. Science *305*, 99–103.

Kim, J., Moody, J.P., Edgerly, C.K., Bordiuk, O.L., Cormier, K., Smith, K., Beal, M.F., and Ferrante, R.J. (2010). Mitochondrial loss, dysfunction and altered dynamics in Huntington's disease. Hum. Mol. Genet. *19*, 3919–3935.

Kitada, T., Asakawa, S., Hattori, N., Matsumine, H., Yamamura, Y., Minoshima, S., Yokochi, M., Mizuno, Y., and Shimizu, N. (1998). Mutations in the parkin gene cause autosomal recessive juvenile parkinsonism. Nature *392*, 605–608.

Knull, H.R. (1978). Association of glycolytic enzymes with particulate fractions from nerve endings. Biochim. Biophys. Acta *522*, 1–9.

Larkman, A.U., Jack, J.J., and Stratford, K.J. (1997). Quantal analysis of excitatory synapses in rat hippocampal CA1 in vitro during low-frequency depression. J. Physiol. *505*, 457–471.

Laughlin, S.B., de Ruyter van Steveninck, R.R., and Anderson, J.C. (1998). The metabolic cost of neural information. Nat. Neurosci. *1*, 36–41.

Leenders, K.L., Perani, D., Lammertsma, A.A., Heather, J.D., Buckingham, P., Healy, M.J., Gibbs, J.M., Wise, R.J., Hatazawa, J., Herold, S., et al. (1990). Cerebral blood flow, blood volume and oxygen utilization. Normal values and effect of age. Brain *113*, 27–47.

Lennie, P. (2003). The cost of cortical computation. Curr. Biol. *13*, 493–497.

Levy, W.B., and Baxter, R.A. (1996). Energy efficient neural codes. Neural Comput. *8*, 531–543.

Levy, W.B., and Baxter, R.A. (2002). Energy-efficient neuronal computation via quantal synaptic failures. J. Neurosci. *22*, 4746–4755.

Li, Z., Okamoto, K., Hayashi, Y., and Sheng, M. (2004). The importance of dendritic mitochondria in the morphogenesis and plasticity of spines and synapses. Cell *119*, 873–887.

Ligon, L.A., and Steward, O. (2000). Role of microtubules and actin filaments in the movement of mitochondria in the axons and dendrites of cultured hippocampal neurons. J. Comp. Neurol. *427*, 351–361.

Lin, M.T., and Beal, M.F. (2006). Mitochondrial dysfunction and oxidative stress in neurodegenerative diseases. Nature *443*, 787–795.

Lin, A.L., Fox, P.T., Hardies, J., Duong, T.Q., and Gao, J.H. (2010). Nonlinear coupling between cerebral blood flow, oxygen consumption, and ATP production in human visual cortex. Proc. Natl. Acad. Sci. USA *107*, 8446–8451.

Lipton, P., and Robacker, K. (1983). Glycolysis and brain function: $[K+]_o$ stimulation of protein synthesis and K^+ uptake require glycolysis. Fed. Proc. *42*, 2875–2880.

Liu, S., Sawada, T., Lee, S., Yu, W., Silverio, G., Alapatt, P., Millan, I., Shen, A., Saxton, W., Kanao, T., et al. (2012a). Parkinson's disease-associated kinase PINK1 regulates Miro protein level and axonal transport of mitochondria. PLoS Genet. *8*, e1002537.

Liu, L., Drouet, V., Wu, J.W., Witter, M.P., Small, S.A., Clelland, C., and Duff, K. (2012b). Trans-synaptic spread of tau pathology in vivo. PLoS ONE *7*, e31302.

Lu, H., Krementsova, E.B., and Trybus, K.M. (2006). Regulation of myosin V processivity by calcium at the single molecule level. J. Biol. Chem. *281*, 31987–31994.

Ma, H., Cai, Q., Lu, W., Sheng, Z.H., and Mochida, S. (2009). KIF5B motor adaptor syntabulin maintains synaptic transmission in sympathetic neurons. J. Neurosci. *29*, 13019–13029.

MacAskill, A.F., Rinholm, J.E., Twelvetrees, A.E., Arancibia-Carcamo, I.L., Muir, J., Fransson, A., Aspenstrom, P., Attwell, D., and Kittler, J.T. (2009). Miro1 is a calcium sensor for glutamate receptor-dependent localization of mitochondria at synapses. Neuron *61*, 541–555.

MacAskill, A.F., Atkin, T.A., and Kittler, J.T. (2010). Mitochondrial trafficking and the provision of energy and calcium buffering at excitatory synapses. Eur. J. Neurosci. *32*, 231–240.

Madsen, P.L., Cruz, N.F., Sokoloff, L., and Dienel, G.A. (1999). Cerebral oxygen/glucose ratio is low during sensory stimulation and rises above normal during recovery: excess glucose consumption during stimulation is not accounted for by lactate efflux from or accumulation in brain tissue. J. Cereb. Blood Flow Metab. *19*, 393–400.

Magrané, J., Sahawneh, M.A., Przedborski, S., Estévez, Á.G., and Manfredi, G. (2012). Mitochondrial dynamics and bioenergetic dysfunction is associated with synaptic alterations in mutant SOD1 motor neurons. J. Neurosci. *32*, 229–242.

Malonek, D., and Grinvald, A. (1996). Interactions between electrical activity and cortical microcirculation revealed by imaging spectroscopy: implications for functional brain mapping. Science *272*, 551–554.

Mangia, S., DiNuzzo, M., Giove, F., Carruthers, A., Simpson, I.A., and Vannucci, S.J. (2011). Response to 'comment on recent modeling studies of astrocyte-neuron metabolic interactions': much ado about nothing. J. Cereb. Blood Flow Metab. *31*, 1346–1353.

Manwani, A., and Koch, C. (2001). Detecting and estimating signals over noisy and unreliable synapses: information-theoretic analysis. Neural Comput. *13*, 1–33.

Maret, S., Faraguna, U., Nelson, A.B., Cirelli, C., and Tononi, G. (2011). Sleep and waking modulate spine turnover in the adolescent mouse cortex. Nat. Neurosci. *14*, 1418–1420.

Markram, H., Lübke, J., Frotscher, M., Roth, A., and Sakmann, B. (1997). Physiology and anatomy of synaptic connections between thick tufted pyramidal neurones in the developing rat neocortex. J. Physiol. *500*, 409–440.

Mathiesen, C., Caesar, K., Thomsen, K., Hoogland, T.M., Witgen, B.M., Brazhe, A., and Lauritzen, M. (2011). Activity-dependent increases in local oxygen consumption correlate with postsynaptic currents in the mouse cerebellum in vivo. J. Neurosci. 31, 18327–18337.

Maurer, I., Zierz, S., and Möller, H.J. (2000). A selective defect of cytochrome c oxidase is present in brain of Alzheimer disease patients. Neurobiol. Aging 21, 455–462.

Mink, J.W., Blumenschine, R.J., and Adams, D.B. (1981). Ratio of central nervous system to body metabolism in vertebrates: its constancy and functional basis. Am. J. Physiol. 241, R203–R212.

Mironov, S.L. (2006). Spontaneous and evoked neuronal activities regulate movements of single neuronal mitochondria. Synapse 59, 403–411.

Mironov, S.L. (2007). ADP regulates movements of mitochondria in neurons. Biophys. J. 92, 2944–2952.

Momiyama, A., Silver, R.A., Hausser, M., Notomi, T., Wu, Y., Shigemoto, R., and Cull-Candy, S.G. (2003). The density of AMPA receptors activated by a transmitter quantum at the climbing fibre-Purkinje cell synapse in immature rats. J. Physiol. 549, 75–92.

Navarrete, A., van Schaik, C.P., and Isler, K. (2011). Energetics and the evolution of human brain size. Nature 480, 91–93.

Newman, L.A., Korol, D.L., and Gold, P.E. (2011). Lactate produced by glycogenolysis in astrocytes regulates memory processing. PLoS ONE 6, e28427.

Nusser, Z.R., Lujan, R., Laube, G., Roberts, J.D.B., Molnar, E., and Somogyi, P. (1998). Cell type and pathway dependence of synaptic AMPA receptor number and variability in the hippocampus. Neuron 21, 545–559.

Panov, A.V., Gutekunst, C.A., Leavitt, B.R., Hayden, M.R., Burke, J.R., Strittmatter, W.J., and Greenamyre, J.T. (2002). Early mitochondrial calcium defects in Huntington's disease are a direct effect of polyglutamines. Nat. Neurosci. 5, 731–736.

Pathak, D., Sepp, K.J., and Hollenbeck, P.J. (2010). Evidence that myosin activity opposes microtubule-based axonal transport of mitochondria. J. Neurosci. 30, 8984–8992.

Pellerin, L., and Magistretti, P.J. (1994). Glutamate uptake into astrocytes stimulates aerobic glycolysis: a mechanism coupling neuronal activity to glucose utilization. Proc. Natl. Acad. Sci. USA 91, 10625–10629.

Perge, J.A., Koch, K., Miller, R., Sterling, P., and Balasubramanian, V. (2009). How the optic nerve allocates space, energy capacity, and information. J. Neurosci. 29, 7917–7928.

Potter, W.B., O'Riordan, K.J., Barnett, D., Osting, S.M., Wagoner, M., Burger, C., and Roopra, A. (2010). Metabolic regulation of neuronal plasticity by the energy sensor AMPK. PLoS ONE 5, e8996.

Prichard, J., Rothman, D.L., Novotny, E.J., Petroff, O.A.C., Kuwabara, T., Avison, M., Howseman, A., Hanstock, C., and Shulman, R.G. (1991). Lactate rise detected by ^{1}H NMR in human visual cortex during physiologic stimulation. Proc. Natl. Acad. Sci. USA 88, 5829–5831.

Puopolo, M., Raviola, E., and Bean, B.P. (2007). Roles of subthreshold calcium current and sodium current in spontaneous firing of mouse midbrain dopamine neurons. J. Neurosci. 27, 645–656.

Rintoul, G.L., Filiano, A.J., Brocard, J.B., Kress, G.J., and Reynolds, I.J. (2003). Glutamate decreases mitochondrial size and movement in primary forebrain neurons. J. Neurosci. 23, 7881–7888.

Rossi, D.J., Oshima, T., and Attwell, D. (2000). Glutamate release in severe brain ischaemia is mainly by reversed uptake. Nature 403, 316–321.

Rouach, N., Koulakoff, A., Abudara, V., Willecke, K., and Giaume, C. (2008). Astroglial metabolic networks sustain hippocampal synaptic transmission. Science 322, 1551–1555.

Rui, Y., Tiwari, P., Xie, Z., and Zheng, J.Q. (2006). Acute impairment of mitochondrial trafficking by beta-amyloid peptides in hippocampal neurons. J. Neurosci. 26, 10480–10487.

Sakata, J.T., and Jones, T.A. (2003). Synaptic mitochondrial changes in the motor cortex following unilateral cortical lesions and motor skills training in adult male rats. Neurosci. Lett. 337, 159–162.

Scharf, M.T., Naidoo, N., Zimmerman, J.E., and Pack, A.I. (2008). The energy hypothesis of sleep revisited. Prog. Neurobiol. 86, 264–280.

Schölvinck, M.L., Howarth, C., and Attwell, D. (2008). The cortical energy needed for conscious perception. Neuroimage 40, 1460–1468.

Scholz, K.P., and Miller, R.J. (1991). Analysis of adenosine actions on Ca^{2+} currents and synaptic transmission in cultured rat hippocampal pyramidal neurones. J. Physiol. 435, 373–393.

Schurr, A., West, C.A., and Rigor, B.M. (1988). Lactate-supported synaptic function in the rat hippocampal slice preparation. Science 240, 1326–1328.

Sengupta, B., Stemmler, M., Laughlin, S.B., and Niven, J.E. (2010). Action potential energy efficiency varies among neuron types in vertebrates and invertebrates. PLoS Comput. Biol. 6, e1000840.

Shahpasand, K., Uemura, I., Saito, T., Asano, T., Hata, K., Shibata, K., Toyoshima, Y., Hasegawa, M., and Hisanaga, S.I. (2012). Regulation of mitochondrial transport and inter-microtubule spacing by tau phosphorylation at the sites hyperphosphorylated in Alzheimer's disease. J. Neurosci. 32, 2430–2441.

Shannon, C.E. (1948). A mathematical theory of communication. Bell Syst. Tech. J. 27, 379–423.

Sheehan, J.P., Swerdlow, R.H., Miller, S.W., Davis, R.E., Parks, J.K., Parker, W.D., and Tuttle, J.B. (1997). Calcium homeostasis and reactive oxygen species production in cells transformed by mitochondria from individuals with sporadic Alzheimer's disease. J. Neurosci. 17, 4612–4622.

Sheng, Z.-H., and Cai, Q. (2012). Mitochondrial transport in neurons: impact on synaptic homeostasis and neurodegeneration. Nat. Rev. Neurosci. 13, 77–93.

Shirendeb, U.P., Calkins, M.J., Manczak, M., Anekonda, V., Dufour, B., McBride, J.L., Mao, P., and Reddy, P.H. (2012). Mutant huntingtin's interaction with mitochondrial protein Drp1 impairs mitochondrial biogenesis and causes defective axonal transport and synaptic degeneration in Huntington's disease. Hum. Mol. Genet. 21, 406–420.

Silver, R.A., Cull-Candy, S.G., and Takahashi, T. (1996). Non-NMDA glutamate receptor occupancy and open probability at a rat cerebellar synapse with single and multiple release sites. J. Physiol. 494, 231–250.

Silver, R.A., Lübke, J., Sakmann, B., and Feldmeyer, D. (2003). High-probability uniquantal transmission at excitatory synapses in barrel cortex. Science 302, 1981–1984.

Sokoloff, L. (1960). The metabolism of the central nervous system in vivo. In Handbook of Physiology, Section I, Neurophysiology, Volume 3, J. Field, H.W. Magoun, and V.E. Hall, eds. (Washington D.C.: American Physiological Society), pp. 1843–1864.

Spruston, N., Jonas, P., and Sakmann, B. (1995). Dendritic glutamate receptor channels in rat hippocampal CA3 and CA1 pyramidal neurons. J. Physiol. 482, 325–352.

Stellwagen, D., and Malenka, R.C. (2006). Synaptic scaling mediated by glial TNF-α. Nature 440, 1054–1059.

Sung, J.Y., Engmann, O., Teylan, M.A., Nairn, A.C., Greengard, P., and Kim, Y. (2008). WAVE1 controls neuronal activity-induced mitochondrial distribution in dendritic spines. Proc. Natl. Acad. Sci. USA 105, 3112–3116.

Suzuki, A., Stern, S.A., Bozdagi, O., Huntley, G.W., Walker, R.H., Magistretti, P.J., and Alberini, C.M. (2011). Astrocyte-neuron lactate transport is required for long-term memory formation. Cell 144, 810–823.

Tanaka, A., Cleland, M.M., Xu, S., Narendra, D.P., Suen, D.F., Karbowski, M., and Youle, R.J. (2010). Proteasome and p97 mediate mitophagy and degradation of mitofusins induced by Parkin. J. Cell Biol. 191, 1367–1380.

Tang, Y., and Zucker, R.S. (1997). Mitochondrial involvement in post-tetanic potentiation of synaptic transmission. Neuron 18, 483–491.

Taylor, K.A. (2007). Regulation and recycling of myosin V. Curr. Opin. Cell Biol. 19, 67–74.

Thompson, J.K., Peterson, M.R., and Freeman, R.D. (2003). Single-neuron activity and tissue oxygenation in the cerebral cortex. Science 299, 1070–1072.

Trushina, E., Dyer, R.B., Badger, J.D., 2nd, Ure, D., Eide, L., Tran, D.D., Vrieze, B.T., Legendre-Guillemin, V., McPherson, P.S., Mandavilli, B.S., et al. (2004). Mutant huntingtin impairs axonal trafficking in mammalian neurons in vivo and in vitro. Mol. Cell. Biol. *24*, 8195–8209.

Turrigiano, G. (2012). Homeostatic synaptic plasticity: local and global mechanisms for stabilizing neuronal function. Cold Spring Harb. Perspect. Biol. *4*, a005736.

Valente, E.M., Abou-Sleiman, P.M., Caputo, V., Muqit, M.M., Harvey, K., Gispert, S., Ali, Z., Del Turco, D., Bentivoglio, A.R., Healy, D.G., et al. (2004). Hereditary early-onset Parkinson's disease caused by mutations in PINK1. Science *304*, 1158–1160.

Vande Velde, C., Garcia, M.L., Yin, X., Trapp, B.D., and Cleveland, D.W. (2004). The neuroprotective factor Wlds does not attenuate mutant SOD1-mediated motor neuron disease. Neuromolecular Med. *5*, 193–203.

Varshney, L.R., Sjöström, P.J., and Chklovskii, D.B. (2006). Optimal information storage in noisy synapses under resource constraints. Neuron *52*, 409–423.

Verstreken, P., Ly, C.V., Venken, K.J., Koh, T.W., Zhou, Y., and Bellen, H.J. (2005). Synaptic mitochondria are critical for mobilization of reserve pool vesicles at Drosophila neuromuscular junctions. Neuron *47*, 365–378.

Vyazovskiy, V.V., Cirelli, C., Pfister-Genskow, M., Faraguna, U., and Tononi, G. (2008). Molecular and electrophysiological evidence for net synaptic potentiation in wake and depression in sleep. Nat. Neurosci. *11*, 200–208.

Wang, X., and Schwarz, T.L. (2009). The mechanism of Ca^{2+} -dependent regulation of kinesin-mediated mitochondrial motility. Cell *136*, 163–174.

Wang, X., Su, B., Lee, H.G., Li, X., Perry, G., Smith, M.A., and Zhu, X. (2009). Impaired balance of mitochondrial fission and fusion in Alzheimer's disease. J. Neurosci. *29*, 9090–9103.

Wang, X., Winter, D., Ashrafi, G., Schlehe, J., Wong, Y.L., Selkoe, D., Rice, S., Steen, J., LaVoie, M.J., and Schwarz, T.L. (2011). PINK1 and Parkin target Miro for phosphorylation and degradation to arrest mitochondrial motility. Cell *147*, 893–906.

Wieraszko, A. (1982). Changes in the hippocampal slices energy metabolism following stimulation and long-term potentiation of Schaffer collaterals-pyramidal cell synapses tested with the 2-deoxyglucose technique. Brain Res. *237*, 449–457.

Wimmer, V.C., Horstmann, H., Groh, A., and Kuner, T. (2006). Donut-like topology of synaptic vesicles with a central cluster of mitochondria wrapped into membrane protrusions: a novel structure-function module of the adult calyx of Held. J. Neurosci. *26*, 109–116.

Wong-Riley, M.T.T. (1989). Cytochrome oxidase: an endogenous metabolic marker for neuronal activity. Trends Neurosci. *12*, 94–101.

Wyss, M.T., Jolivet, R., Buck, A., Magistretti, P.J., and Weber, B. (2011). In vivo evidence for lactate as a neuronal energy source. J. Neurosci. *31*, 7477–7485.

Xu, H.-T., Pan, F., Yang, G., and Gan, W.-B. (2007). Choice of cranial window type for in vivo imaging affects dendritic spine turnover in the cortex. Nat. Neurosci. *10*, 549–551.

Youle, R.J., and Narendra, D.P. (2011). Mechanisms of mitophagy. Nat. Rev. Mol. Cell Biol. *12*, 9–14.

Zador, A. (1998). Impact of synaptic unreliability on the information transmitted by spiking neurons. J. Neurophysiol. *79*, 1219–1229.

Zador, A.M. (2001). Synaptic connectivity and computation. Nat. Neurosci. *4*, 1157–1158.

Zhang, C.L., Ho, P.L., Kintner, D.B., Sun, D., and Chiu, S.Y. (2010). Activity-dependent regulation of mitochondrial motility by calcium and Na/K-ATPase at nodes of Ranvier of myelinated nerves. J. Neurosci. *30*, 3555–3566.

Zhu, Y.B., and Sheng, Z.H. (2011). Increased axonal mitochondrial mobility does not slow amyotrophic lateral sclerosis (ALS)-like disease in mutant SOD1 mice. J. Biol. Chem. *286*, 23432–23440.